The emergence of a polar nematic phase: a chemist's insight into the ferroelectric nematic phase.
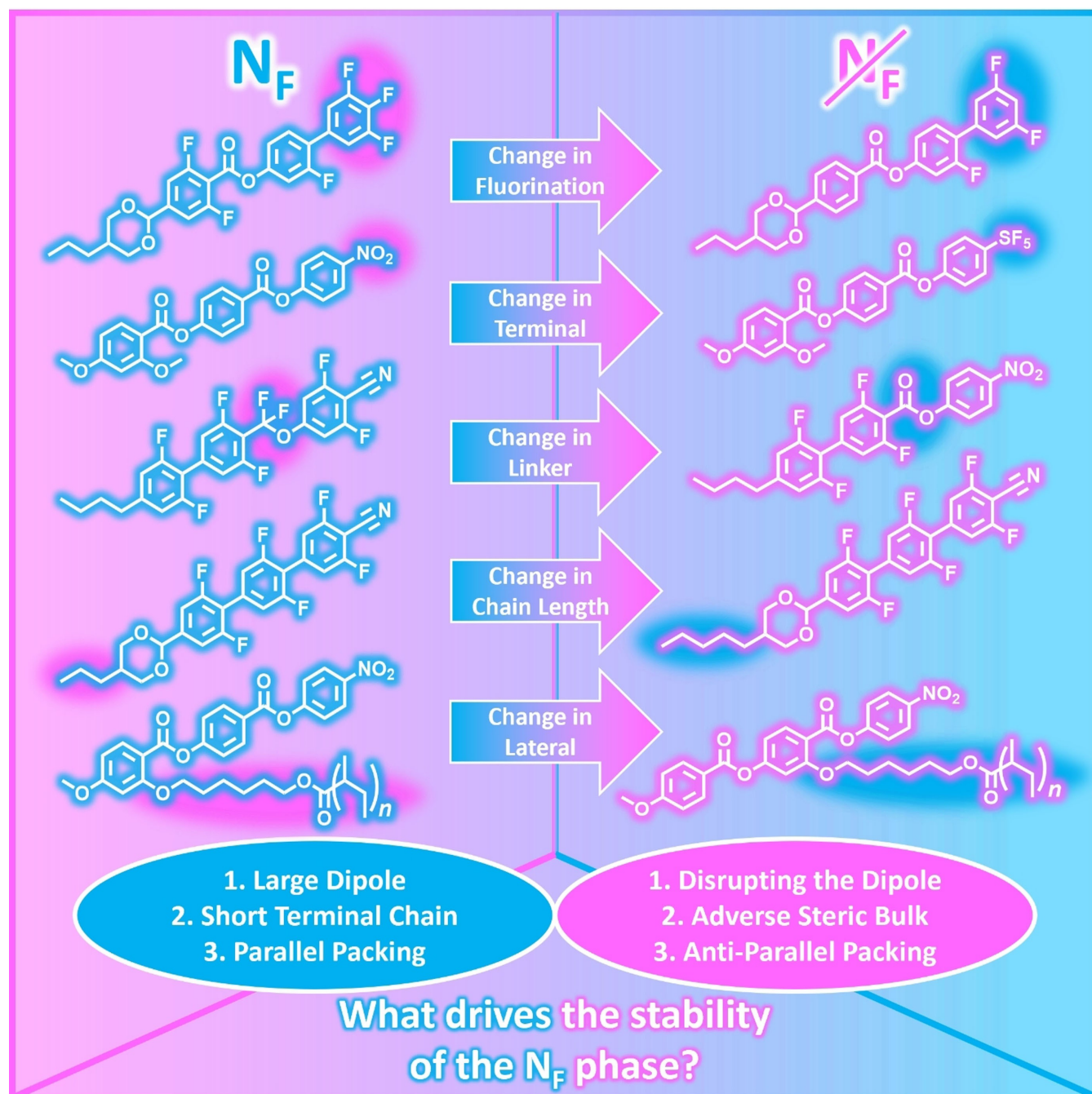
CRUICKSHANK, E.

2024

ChemPlusChem

Review
doi.org/10.1002/cplu.202300726

Chemistry Europe
European Chemical
Societies Publishing

www.chempluschem.org

The Emergence of a Polar Nematic Phase: A Chemist's Insight into the Ferroelectric Nematic Phase

Ewan Cruickshank*[a]

The discovery of a new polar nematic phase; the ferroelectric nematic, has generated a great deal of excitement in the field of liquid crystals. To date there have been around 150 materials reported exhibiting the ferroelectric nematic phase, in general, following three key archetypal structures with these compounds known as RM734, DIO and UUQU-4N. In this review, the relationship between the molecular structure and the stability of the ferroelectric nematic, N_F, phase will be described from a chemist's perspective. This will look to highlight the wide variety of functionalities which have been incorporated into these archetypal structures and how these changes influence the transition temperatures of the mesophases present. The N_F phase appears to be stabilised particularly by reducing the length of terminal alkyl chains present and adding fluorines laterally along the length of the molecular backbone. This review will look to introduce the background of the ferroelectric nematic phase before then showing the molecular structures of a range of materials which exhibit the phase, describing their structure–property relationships and therefore giving an up–to–date account of the literature for this fascinating new mesophase.

1. Introduction

The conventional nematic phase, N, has been ubiquitous with the development of liquid crystal display technology since the discovery of the *n*CB series by George Gray in the early 1970s.[1] It has been technologically the most important liquid crystalline phase, or mesophase, underpinning the multibillion dollar liquid crystal display market. The conventional nematic phase is the least ordered mesophase, in which the long axes of the rod–like molecules are aligned in more–or–less the same direction known as the director, **n**, Figure 1. The centres of masses of the rod–like molecules are randomly distributed and the phase is non–polar in nature. This is because of the inversion symmetry present within the phase meaning that $\mathbf{n} = -\mathbf{n}$. While some features of the conventional nematic phase are maintained in the ferroelectric nematic phase, N_F, critically, the inversion symmetry that was present is broken such that $\mathbf{n} \neq -\mathbf{n}$ and therefore the phase is polar, Figure 1.

The concept of a polar nematic phase can hardly be described as new, having been speculated upon as early as 1916 by Max Born who attempted to develop a mathematical theory for liquid crystals. He suggested that a polar fluid would exist if the dipoles of the constituent molecules were sufficiently large that the dipole–dipole interactions between them could overcome thermal fluctuations.[2] An underlying assumption within the model, that molecules had to possess a dipole moment before they could form any liquid crystalline phases, was proven to be incorrect by the emergence of non–polar molecules which were liquid crystalline.[3] It was even commented on in a review of the history of liquid crystals that the theory proposed by Born had been 'relegated to the status of a historical footnote'.[4] However, some 100 years after Born's work, a polar nematic phase was finally experimentally observed in 2017. The phase was first reported by two independent groups in the molecules RM230,[5] RM734[6] and DIO,[7] Figure 2, although at the time they were described as

having what appeared to be multiple nematic phases rather than specifically the ferroelectric nematic phase. In 2020, however, when studying RM734, Chen *et al.* demonstrated that the additional nematic phase present was in fact ferroelectric and named this phase the ferroelectric nematic phase.[8] The discovery of the N_F phase has seen a flurry of activity in this area and the phase has rapidly become arguably the hottest topic in liquid crystals. There is a good reason for this excitement around the phase, and that is because it shows a range of unique and interesting properties. Indeed, these include some which mean that the phase may have real application potential. Some of these properties include: being easy to align;[9,10] having a strong non-linear optical response;[11–15] high polarisation values;[7,8,16,17] large dielectric permittivity[18–26] (although there has been some debate around the exact magnitude of these permittivity values)[26,27] and switching occurs for very low electric fields.[7,8,20,28–33]

While there has been a large upsurge in materials in the last couple of years that have been reported to exhibit the ferroelectric nematic phase, the majority of these compounds fall into a relatively small structure space. Indeed, bar a few examples which will be discussed, most N_F compounds can be classified into three general archetypal structures which are based on the molecules RM734,[6] DIO[7] and UUQU-4N,[24] Figure 2. While their structures appear chemically to be somewhat different in nature, there does appear to be some features which are similar in all three materials. Firstly, these materials all possess a large longitudinal dipole moment which can drive the favourable interactions between the molecules required to observe the N_F phase. Secondly, these materials all have some degree of lateral bulk, whether that is in the form of an alkyloxy chain or lateral fluorination, and this is thought to inhibit the anti–parallel correlations that are often associated with low molar mass mesogens and are destabilizing for the N_F phase. These rather empirical observations do have some basis in theory as they are in good accord with the computer simulations reported by Berardi et al.,[34,35] who modelled tapered molecules using a generalized Gay–Berne type of attractive–repulsive potential. The tapered molecules could exhibit a polar nematic phase which has been since described as the N_F phase due to a balance between shape and attractive terms. Relatively small molecular changes to these archetypal materials have led to the development of a library of around 150 ferroelectric nematogens, most of which can be described

[a]   Dr. E. Cruickshank
    School of Pharmacy and Life Sciences, Robert Gordon University, Aberdeen,
    AB10 7GJ, UK
    E-mail: e.cruickshank2@rgu.ac.uk

ChemPlusChem

Review
doi.org/10.1002/cplu.202300726

Chemistry Europe
European Chemical
Societies Publishing

as low molar mass mesogens.[6,14,36–42,18–21,24,30,31,33] While there have been exceptions to these archetypal materials,[25,41,43,44] these have been quite limited and so there is still a great deal of understanding that can be gained in terms of structure–property relationships involved in the formation of the N_F phase. This has been highlighted recently by reports of DIO–based molecules also exhibiting a ferroelectric smectic A phase, Figure 1.[31,38,45] For many of the materials reviewed here, the polar character of the N_F phase was described by the appearance of a strong dielectric relaxation mode,[14,19–21,24,25,33] the exact magnitude of which, as was mentioned previously, has come under some discussion recently,[27] but this review will not look to resolve this and will use the phase sequences as they have been reported in the literature. The other method used in the determination of the N_F phase was polarised optical microscopy and the observation of characteristic banded textures, with examples of these shown in Figure 3. This review will instead look to summarise some of the structural modifications made to the materials exhibiting the N_F phase, from a chemist's perspective, and will look to summarise what effect these changes have had on the stability of the N_F phase. For clarity, some of the compounds listed were initially reported as the N_S phase, however,[11,23,46,47] with RM734 being assigned as the N_F phase,[8] that is the nomenclature which will be used throughout. The compounds in this review will be labelled numerically in sequence for clarity, rather than using the nomenclature provided in the literature they are referenced from. This work also looks to add additional insights into the N_F phase following on from the excellent reviews on the subject by Mandle[39] and Sebastián et al.[40]

2. Materials Based on DIO

DIO, as was mentioned earlier, is one of the archetypal materials which exhibits the ferroelectric nematic phase. DIO has a structure characterised by a dioxane ring at one terminus and a fluorinated biphenyl at the other joined by an ester linking group which gives the molecule a large longitudinal dipole, calculated to be 9.4 D,[7,48] and as was described previously this appears to be required for the N_F phase to form. The calculation of the molecular dipole in these types of compounds have

Dr Ewan Cruickshank is a Lecturer in the School of Pharmacy and Life Sciences at Robert Gordon University. Prior to joining RGU in 2023, he was a research fellow at the University of Aberdeen where he worked on the EPSRC funded New Horizons project: Ferroelectricity and the Nematic Liquid Crystal Phase. His PhD was completed at the University of Aberdeen where his thesis titled: Synthesis and Characterisation of Novel Thioether–Based Liquid Crystals and the Twist–Bend Nematic Phase was sustained in 2021. He was awarded the Luckhurst–Samulski Prize in 2019 for the best paper that year in the journal Liquid Crystals.

been widely undertaken using density functional theory, however, in order to account for the different basis sets used, the calculation method for each dipole has been reported in the footnotes of the tables. DIO much like other N_F materials has been reported to have a large polarisation value, in the case of DIO, 4.4 µC cm^{-2}.[7,8] DIO, labelled compound **1**, shows a phase sequence on cooling of I–174 °C–N–84 °C–N_X–69 °C–N_F and it will be used as the baseline N_F transition temperature which the other materials will be compared to. The N_X phase listed here has been subsequently called the SmZ_A phase and the proposed structure of this phase has been described in literature by Chen et al.[49] and later confirmed by Cruickshank et al.,[50] Figure 4.

They suggested that the phase has only short–range order regarding molecular positions but shows a regular array of antiferroelectric domains along the direction perpendicular to the director. These regular domains give a kind of long–range periodicity, and this led to very weak Bragg–type diffraction signals being measured, and hence being referred to as the antiferroelectric SmZ_A phase. Cruickshank et al.,[50] however, suggested that the origin of the detected diffraction signal is not the packing of the molecules into distinct layers, but instead the nematic order within the blocks. They, therefore, differentiated this phase from regular smectic phases and instead kept its identification as a nematic phase. The phase was referred to as the N_X phase and will be the terminology used in this review for this phase. The modifications to the structure will start as small individual changes but these will quickly increase in complexity. Firstly, looking at the effect of changing the substituents on the middle monofluorinated aromatic ring, Table 1.[18,19] In Table 1 and elsewhere the liquid crystal phase sequences are given on cooling to keep consistency between the molecules. In order to highlight that most of the N_F phase transitions were monotropic in nature and require supercooling, the melting points of the compounds have been listed where available. Li et al. reported that removing the fluorine meta to the ester saw the N_F phase completely destabilised despite the material maintaining a large longitudinal dipole moment and the replacement of the fluorine atom by a lateral methoxy group saw the N_F phase destabilised by 3 °C. Increasing the length of the methoxy group in this position to ethoxy, propoxy and butoxy, compounds **3.2**–**3.4**, again saw the N_F phase completely destabilised. The addition of a second fluorine substituent meta to the ester of the middle aromatic ring sees the N_F phase greatly stabilised with T_{NFN} increasing by 55 °C. While this may appear to suggest that merely increasing the magnitude of the molecular dipole will also increase the stability of the N_F phase, it will become clear that this is an overly simplistic view.

There have also been changes made to the trifluorinated terminal aromatic ring, specifically replacing the central fluorine of the three, para to the bond to the other aromatic ring, with other polar functional groups, Table 2.[45,48] Nishimura et al.[48] reported that substituting the aforementioned fluorine with a CF_3 group saw the N_F phase stabilised by 39 °C and the dipole moment increased to 11.0 D. Interestingly, the inclusion of this group also saw the emergence of a phase which the authors
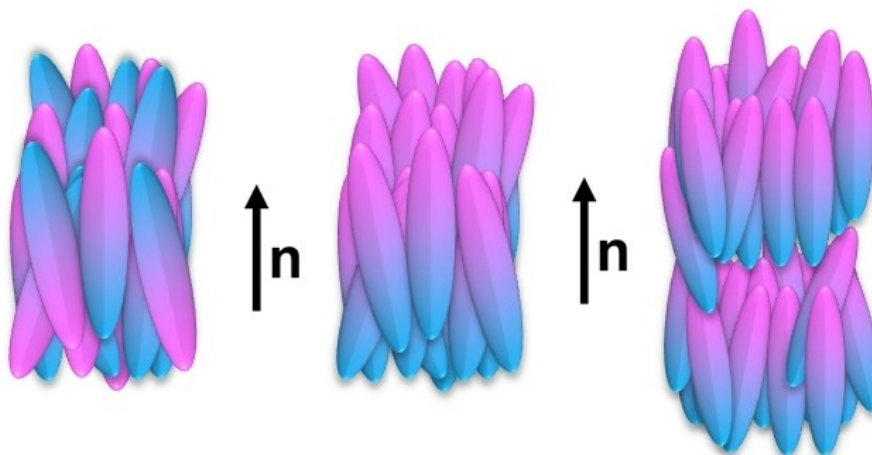
ChemPlusChem

Review
doi.org/10.1002/cplu.202300726

**Chemistry
Europe**
European Chemical
Societies Publishing

Figure 1. Schematic representations of the: (left) conventional nematic phase, (middle) ferroelectric nematic phase and (right) ferroelectric smectic A phase.
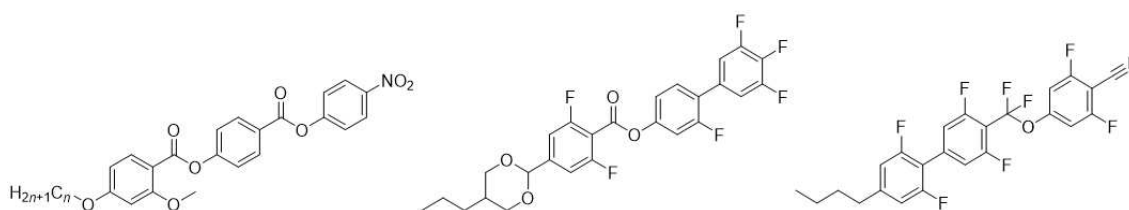

Figure 2. Molecular structures of archetypal ferroelectric nematogens: (left) RM734 when $n = 1$ and RM230 when $n = 2$, (middle) DIO and (right) UUQU-4 N.

labelled as being smectic preceding the N_F phase. Considering the transition temperature for this phase was higher than that of the N_F phase, it can be presumed that this phase was the N_X phase, which was described earlier. Matsukizono *et al.*[45] reported that replacing the fluorine with a hydrogen, compound **6**, saw the N_F phase be completely destabilised similarly to what was seen in terms of the middle aromatic ring of DIO. Replacing that fluorine instead with a cyano moiety, compound **7**, saw the N_F phase maintained with a decrease in the transition temperature of 4 °C compared to DIO and the

emergence of a second polar nematic phase that the authors termed N'_F. They differentiated this phase from the conventional N_F phase because there was a change in the polarisation value of the phase, but the *D–E* curve still showed a large hysteresis indicative of its ferroelectric properties. This decrease is somewhat surprising considering the same material was reported by Li *et al.*[19] with a transition to the N_F phase at 129 °C, Matsukizono *et al*[45] suggested that the transition at 129 °C is to the N_X phase rather than the N_F phase and this was supported by the dielectric constants measured in this phase.
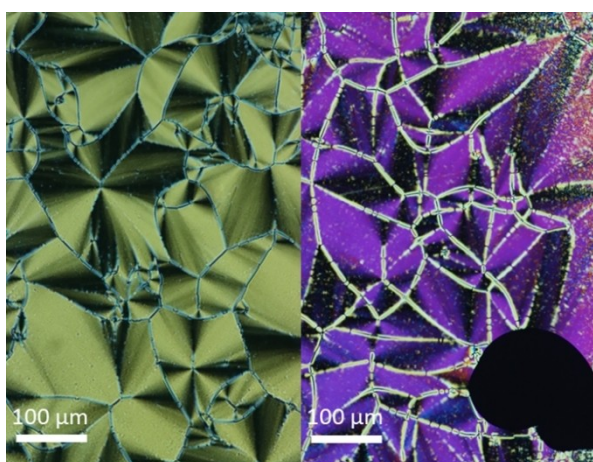
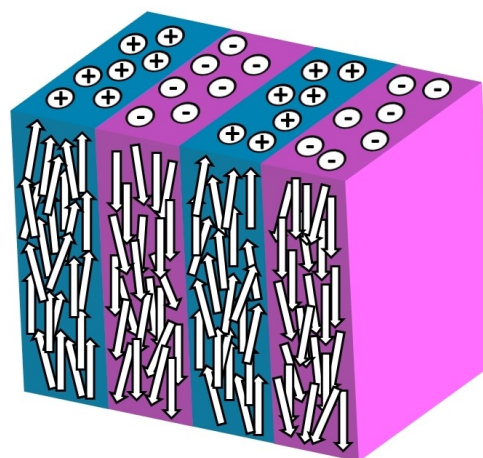**Figure 3.** Representative examples of the banded textures observed for the ferroelectric nematic phase.

Figure 4. Schematic representation of the N_X phase, with the arrows representing the molecular dipoles and the point of the arrow marking the end of the molecule with a positive charge.

Table 1. The molecular structures, phase sequences and average dipole moments of compounds **1**–**4**.

Compound		Structure	Melting Point/°C	Phase Sequence/°C	ΔT_{NF}/°C	μ/ D	Ref.
1			96	I–174–N–85–N_X–69–N_F–34–Cr	–	9.4[a]	7,21
2			–	I–120–N	×	8.4[b]	18
3	1		–	I–91–N–66–N_F–47–Cr	−3	8.4[b]	18
	2		–	I–59–Cr	×	10.1[b]	19
	3		–	I–48–Cr	×	10.0[b]	19
	4		–	I–39–Cr	×	10.0[b]	19
4			–	I–147–N–124–N_F	+55	9.4[b]	18

[a] Calculated using B3LYP/6-31G (d). [b] Calculated using B3LYP/6-311+G(d,p).
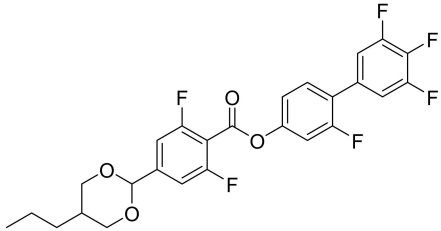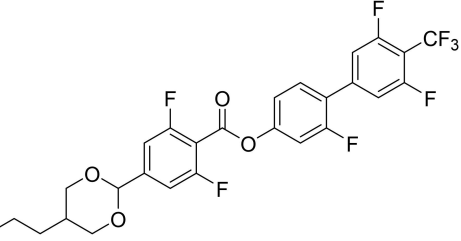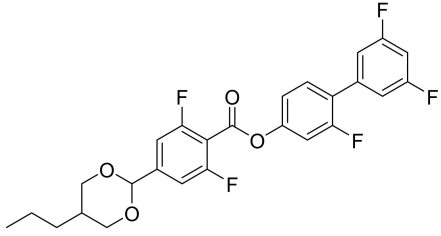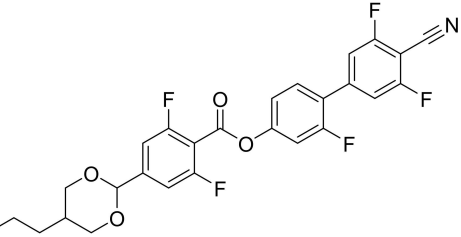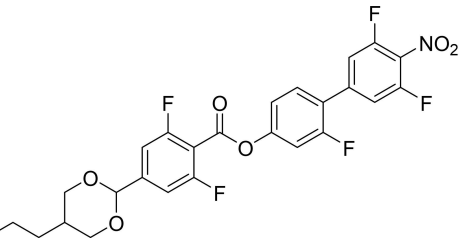
They also described the N′$_F$ phase being present in this compound, but in this case T_{NFNX} increased by 27 °C compared to DIO, suggesting that a terminal nitro group is favourable for the observation of the N_F phase.

The extent and position of fluorination can also be altered for the terminal aromatic ring connected to the dioxane ring, Table 3[38,45] Kikuchi *et al.* showed that removing one or both of the fluorine atoms from the terminal aromatic ring connected to the dioxane ring saw the N_F phase replaced by a ferroelectric smectic phase. The transition to the SmA_F phase was seen at 106 °C for the ring with a single fluorine, compound **9**, and at 146 °C when there were no fluorines, compound **10.3**. The dielectric measurements and observed POM textures suggested that the lowest temperature phase in compound **10.3** was the same as the SmA_F phase in compound **9**, the material with one fluorine in the terminal ring connected to the dioxane ring. The authors also reported, in both compounds **9** and **10.3**, additional smectic phases which had ferroelectric character, and this was based on there being differences in the dielectric measure-

ments between the phases. Nishikawa *et al.*[51] reported that replacing the terminal alkyl chain with a hydrogen, compound **10.0**, the SmA_F phase is still observed but the conventional nematic phase i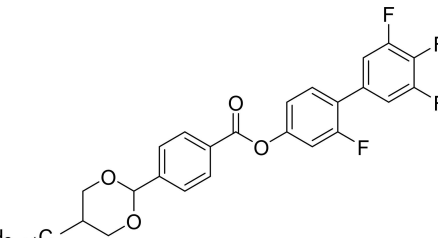s extinguished so the transition is direct from the isotropic phase. Kikuchi *et al.*[38] also reported that changing one of the fluorine positions from 2,6-difluorophenyl to 3,6-difluorophenyl or 2,3-difluorophenyl would also see the complete destabilisation of the N_F phase. This was attributed to the large decrease in the magnitude of the average molecular dipole going from 9.4 D in DIO to 8.13 D and 8.31 D for compounds **11** and **12**, respectively. Similarly replacing the fluorine with a single chlorine also saw the N_F phase being lost, as might be expected, but there was also no observation of the SmA_F phase suggesting that the additional bulk associated with the chlorine also inhibited the formation of smectic phases.

In Table 4 the degree of fluorination in all three of the aromatic rings is varied compared to DIO. In all three compounds the N_F phase is extinguished with the decrease in fluorination, however, compounds **14** and **15** did exhibit a

ChemPlusChem

Review
doi.org/10.1002/cplu.202300726

Chemistry
Europe
European Chemical
Societies Publishing

Table 2. The molecular structures, phase sequences and average dipole moments of compounds **5–8**.

Compound	Structure	Melting Point/°C	Phase Sequence/°C	ΔT_{NF}/°C	μ/D	Ref.
1	(chemical structure)	96	I–174–N–85–N_X–69–N_F	–	9.4[a]	7,21
5	(chemical structure)	–	I–168–N–118–N_X–108–N_F–86–Cr	+39	11.0[b]	48
6	(chemical structure)	74	I–132–N	×	11.2[c]	45
7	(chemical structure)	121	I–244–N–130–N_X–65–N_F–58–N_F'	−4	13.4[c]	45
8	(chemical structure)	98	I–184–N–117–N_X–96–N_F–92–N_F'	−27	13.0[c]	45
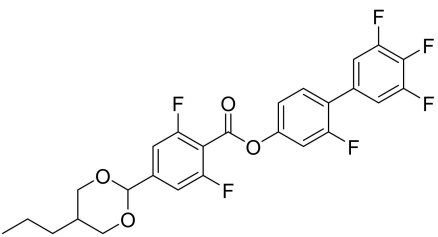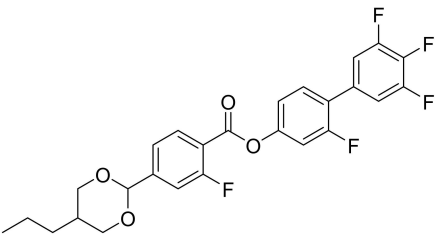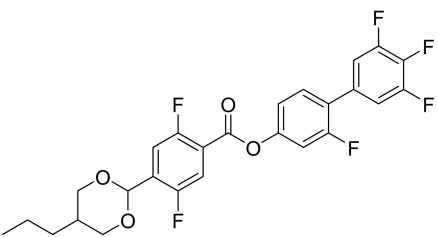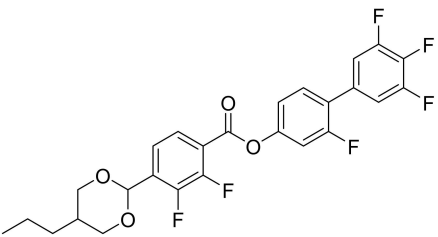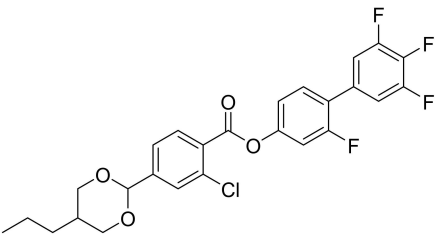
[a] Calculated using B3LYP/6-31G (d). [b] Calculated using ωB97X–D/6-311G (d,p). [c] Calculated using B3LYP/6-31+G(2d,p).

smectic phase that appeared to be conventional albeit without a clear assignment. Most of the convenient or simple modifications that can be made to these structures destabilise the N_F phase. Also included in Table 4, are compounds **17** and **18** reported by Nishimura *et al.*[48] who replaced the dioxane ring with a butoxy terminal chain and a dimethylamino group, respectively. Compound **17** had 2 fluorines *meta* to the terminal butoxy chain whereas compound **18** had no fluorination at those positions, both compounds, however, did not exhibit the N_F phase. Nishimura *et al.*[48] also reported compound **19** with

the dioxane ring replaced by a cyclohexane moiety and a pentyl terminal chain. Li *et al.*[18] reported compound **20** which had a similar molecular design to compound **18** but with a methoxy terminal chain. However, neither of these materials exhibited the N_F phase.

Li *et al.* reported a wide variety of DIO based compounds with differing terminal chain lengths, polar end groups and functionality substituted onto the aromatic rings as is summarised in Table 5.[19] There is a general trend that can be observed from these materials in terms of the length of the terminal

Table 3. The molecular structures, phase sequences and average dipole moments of compounds **9–13**.

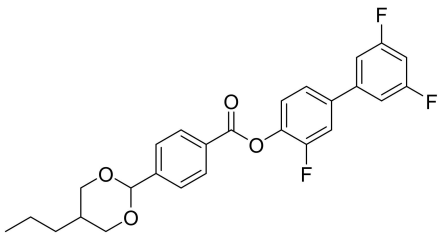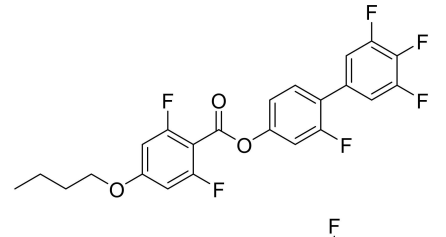| Compound		Structure	Melting Point/ °C	Phase Sequence/°C	ΔT_{NF}/ °C	μ/D	Ref.
1			96	I–174–N–85–N_X–69–N_F–34–Cr	–	9.4[a]	7,21
9			107	I–207–N–115–N_X–106–SmA_F–85–SmX_F	×	9.4[b]	38
10	0		153	I–148–SmA_F–117–SmX_F–105–Cr	×	9.0[c]	51
	3		129	I–231–N–158–SmA_F'–146–SmA_F	×	8.7[b]	38
11			123	I–196–N	×	8.4[b]	38,45
12			126	I–180–N	×	8.4[b]	38,45
13			72	I–137–N	×	9.2[b]	38

[a] Calculated using B3LYP/6-31G (d). [b] Calculated using B3LYP/6-31+G(2d,p). [c] Calculated using B3LYP/6-311+G(d,p).

chain, which is that the shorter the chain length the greater the stability of the N_F phase. This can be seen with series **22–26** and **28**, despite the different lateral and terminal groups introduced into the terminal biphenyl rings. Although it must be noted that compounds **21** and **22.0**, which have a hydrogen replacing the terminal alkyl chain, sees the N_F phase extinguished and T_{NFI}

ChemPlusChem

Review

doi.org/10.1002/cplu.202300726

Chemistry Europe
European Chemical
Societies Publishing

Table 4. The molecular structures, phase sequences and average dipole moments of compounds **14–20**.
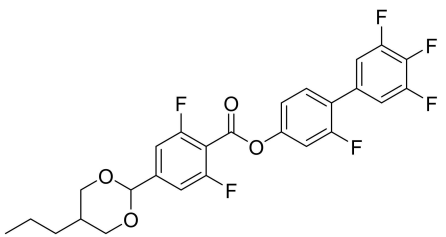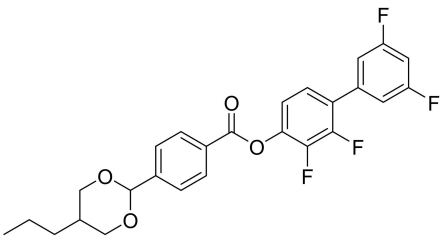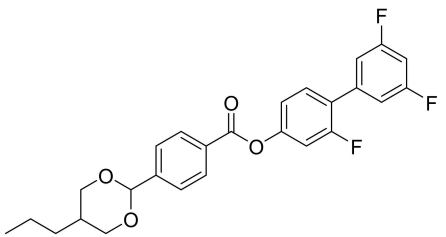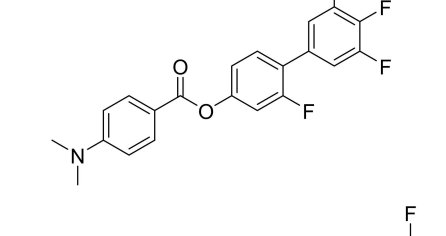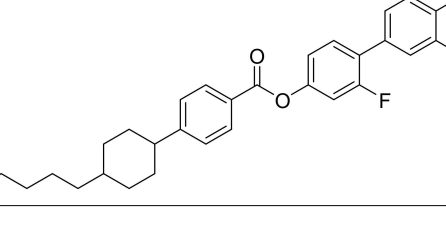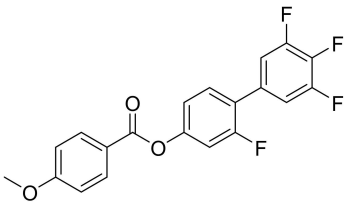
Compound	Structure	Melting Point/°C	Phase Sequence/°C	ΔT$_{NF}$/°C	μ/D	Ref.
1		96	I–174–N–85–NX–69–NF–34–Cr	–	9.4[a]	7,21
14		128	I–186–N–84–SmX	×	6.9[b]	45
15		124	I–185–N–147–SmX	×	8.2[b]	45
16		122	I–194–N	×	5.9[b]	45
17		98	I–112–N	×	8.2[c]	48
18		189	I–164–Cr	×	5.9[c]	48
19		117	I–233–N–129–Sm	×	6.4[b]	45

Table 4. continued						
Compound	Structure	Melting Point/°C	Phase Sequence/°C	ΔT_{NF}/°C	μ/D	Ref.
20		–	I–134–N–92–Cr	×	6.8[d]	18

[a] Calculated using B3LYP/6-31G(d). [b] Calculated using B3LYP/6-31+G(2d,p). [c] Calculated using ωB97X–D/6-311G(d,p). [d] Calculated using B3LYP/6-311+G(d,p).

decrease by 4 °C compared to compound **22.1**, respectively. While the materials with the methyl terminal chains attached to the dioxane ring have the lowest average molecular dipoles of each of the series that they are in, this seems to be favourable for the stability of the N_F phase. Indeed, all the compounds with the shortest terminal chain lengths exhibit the N_F phase, some even showing a direct N_F–I transition, and this is not the case for those with longer terminal chains. Having a shorter terminal chain means that there will be less electron density inductively donated to the 2,6-difluorinated aromatic ring. This observation is consistent with the predictions of a molecular model developed by Madhusudana to describe the N_F phase.[52] Within the framework of the model, the calamitic molecules are represented by regions of alternating positive and negative charges separated by the ester group and dictated by the electron–withdrawing or donating nature of the functional groups substituted onto the aromatic rings, Figure 5. The terminus of the rod with the dioxane ring is positively charged and the other is negative, which gives the large longitudinal dipole moment. If these rods exist in close proximity, then the neighbouring molecules are sensitive to the electronic charge of each other and these interactions inhibit the formation of anti–parallel structures, Figure 5. Specifically, this suggests that
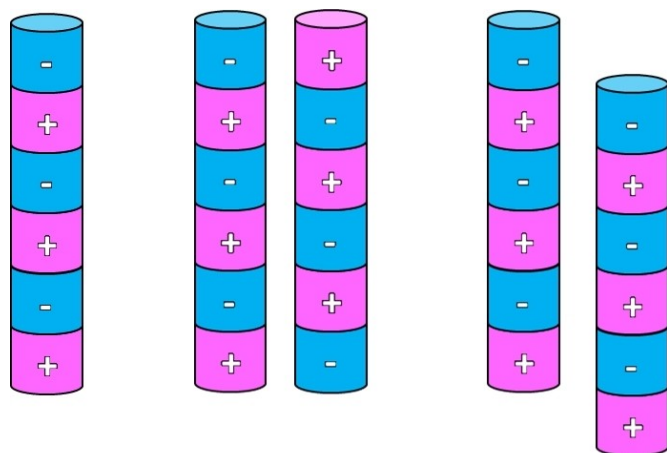
the parallel alignment of the molecules, Figure 5, is enhanced by minimising the amplitude of the charge density wave at either end of the molecule and this is achieved in this case by reducing the length of the alkyl chain. However, the opposite is the case when the chain length is increased: the stability of the N_F phase is diminished even to the extent that for some of the series it is extinguished. It would be remiss not to highlight compound **25.1** which shows a direct N_F–I transition at 226 °C which is over 150 °C higher than DIO and one of the highest N_F transition temperatures reported to date. The other structural features which led to this very stable N_F phase will be discussed later.

By comparing the materials with a terminal chain beyond the dioxane ring, which is three carbons long, the effect of the other modifications to the structure can be isolated from the influence of changing the terminal alkyl chain and directly compared to the archetypal compound DIO, Table 5. In compound **22.3**, the fluorine atom *meta* to the ester is substituted for a polar nitro group and there is, as might be expected, an increase in the average molecular dipole of around 2 D. However, the additional lateral bulk associated with the nitro group mitigates the enhanced polarity it brings such that the N_F phase is slightly destabilised compared to DIO, seeing T_{NFN} drop by 3 °C. In compounds **23.3** and **24.3**, which have terminal nitro groups the N_F phase is completely destabilised and only a conventional nematic phase is observed. This maybe slightly surprising given both compounds **23.1** and **24.1** show an increase in the stability of the N_F phase compared to compound **22.1**. While both compounds **23.3** and **24.3** have enhanced dipoles when compared to DIO at 12.2 D and 13.2 D respectively, the removal of the fluorines *ortho* to the terminal nitro group is presumably unfavourable for the parallel packing of the molecules as the terminal chain length increases and hence why the N_F phase is not observed. Replacing the central terminal fluorine with a cyano group and adding an additional fluorine *meta* to the ester as seen in compound **25.3**, sees a remarkable increase in the stability of the N_F phase with T_{NFNX} increasing by 107 °C in relation to DIO and with the average dipole moment increasing to 14.6 D. Normally introducing a cyano group to a biphenyl would see a promotion in anti–parallel correlations between the mesogenic units and so would see the N_F phase be destabilised. However, in this case, the N_F

Figure 5. Schematic representation of (left) a rod–like molecule with alternating charge, (middle) the molecules orientated in an anti-parallel manner and (right) the molecules orientated in a parallel manner.

ChemPlusChem

Review
doi.org/10.1002/cplu.202300726

Chemistry Europe
European Chemical
Societies Publishing

Table 5. The molecular structures, phase sequences and average dipole moments of compounds **21–37**.
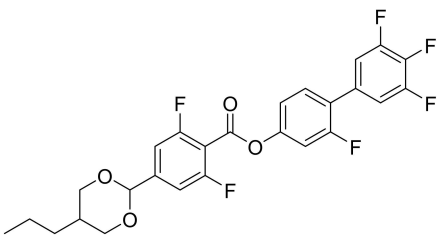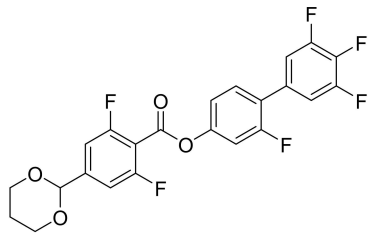
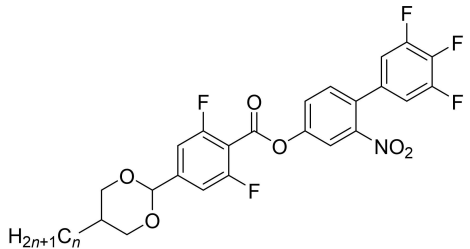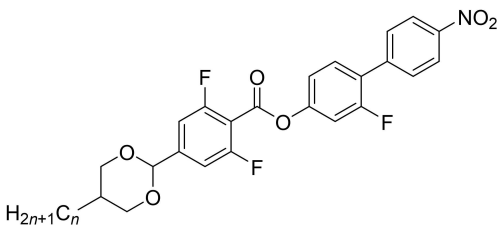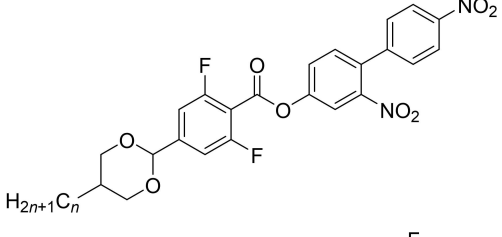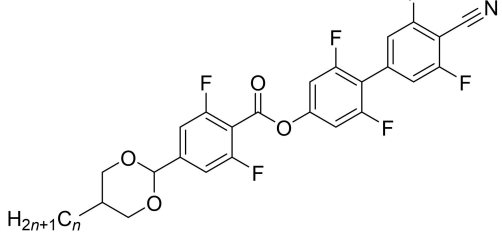| Compound		Structure	Melting Point/°C	Phase Sequence/°C	ΔT_{NF}/°C	μ/D	Ref.
1			96	I–174–N–85–N$_X$–69–N$_F$–34–Cr	–	9.4[a]	7,21
21			144	I–124–Cr	–	9.9[b]	51
22	0		135	I–83–N$_F$–67–Cr	+14	12.2[b]	51
	1		–	I–87–N$_F$	+18	11.2[b]	19
	2		–	I–65–N$_F$–63–Cr	−4	11.3[b]	19
	3		–	I–68–N$_F$	−3	11.4[b]	19
	5		–	I–63–N	×	11.5[b]	19
23	1		–	I–243–N–119–N$_F$–100–Cr	+50	12.0[b]	19
	2		–	I–265–N–56–Cr	×	12.2[b]	19
	3		–	I–270–N–22–Cr	×	12.2[b]	19
	5		–	I–240–N–35–Cr	×	12.3[b]	19
24	1		–	I–120–N$_F$–101–Cr	+51	13.0[b]	19
	2		–	I–120–N–58–Cr	×	13.1[b]	19
	3		–	I–163–N–74–Cr	×	13.2[b]	19
	5		–	I–152–N	×	13.2[b]	19
25	1		–	I–226–N$_F$–140–Cr	+157	14.4[b]	19
	3		–	N–189–N$_X$–175–N$_F$–115–SmA$_F$–65–Cr	+107	14.6[b]	19,31
	5		–	I–218–N–104–N$_F$–28–Cr	+35	14.8[b]	19
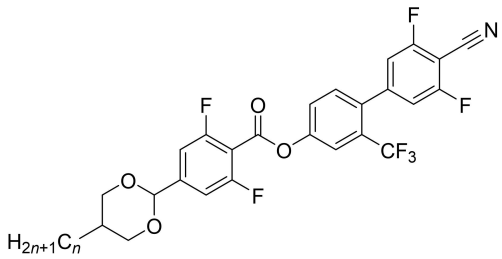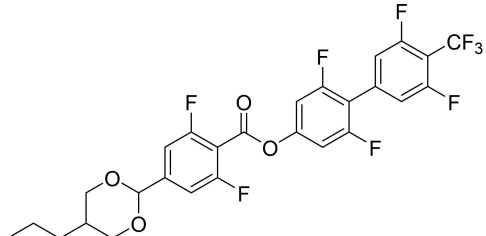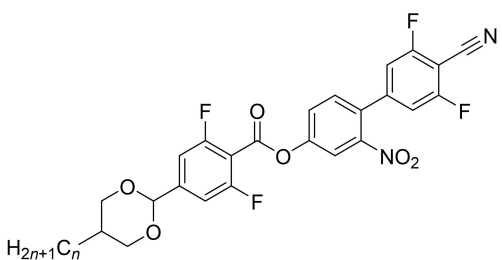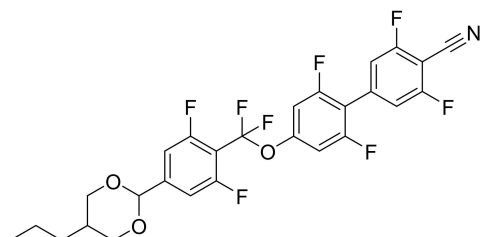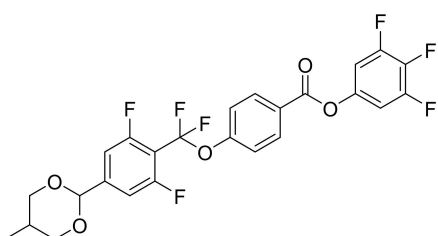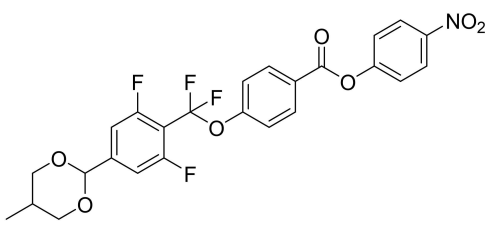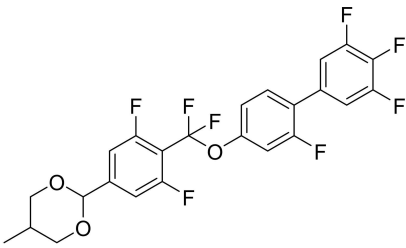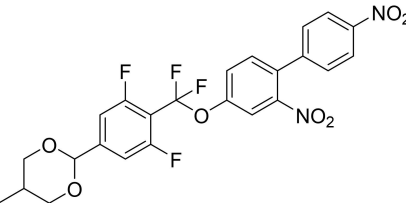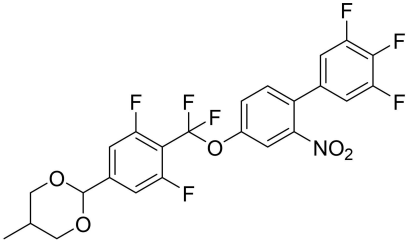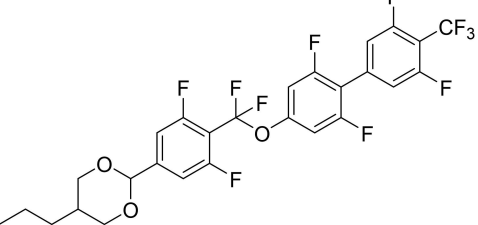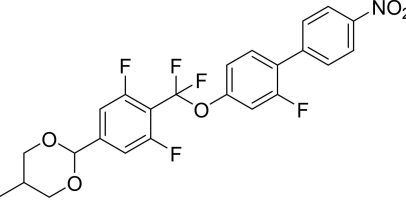
ChemPlusChem

Review
doi.org/10.1002/cplu.202300726

Chemistry
Europe
European Chemical
Societies Publishing

Table 5.	continued						
Compound		Structure	Melting Point/°C	Phase Sequence/°C	ΔT_{NF}/°C	μ/D	Ref.
26	1		–	I–91–N_F	+22	13.8[b]	19
	3		–	I–113–N–86–N_F	+17	14.0[b]	19
	5		–	I–111–N–55–N_F	−14	14.1[b]	19
27			–	I–155–N–138–N_F–113–Cr	+69	12.8[b]	19
28	0		135	I–151–N_F–21–G	+82	14.9[b]	51
	3		–	I–157–N–126–N_F	+57	14.7[b]	19
29			–	I–132–N–96–N_F–22–Cr	+27	13.9[b]	19
30			–	I–50–Cr	×	9.1[b]	18
31			–	I–111–Cr	×	9.7[b]	18

ChemPlusChem

Review
doi.org/10.1002/cplu.202300726

Chemistry
Europe
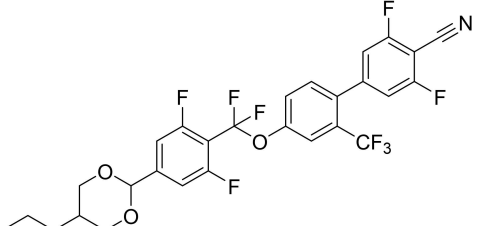European Chemical
Societies Publishing

Table 5. continued

Compound	Structure	Melting Point/°C	Phase Sequence/°C	ΔT_{NF}/°C	μ/D	Ref.
32		–	I–79–Cr	×	7.9[b]	18
33		–	I–85–Cr	×	13.1[b]	19
34		–	I–44–Cr	×	13.5[b]	19
35		–	I–44–Cr	×	11.5[b]	19
36		–	I–71–Cr	×	12.1[b]	19
37		–	I–132–N–80–Cr	×	11.7[b]	19

[a] Calculated using B3LYP/6-31G (d). [b] Calculated using B3LYP/6-311+G(d,p).

phase was stabilised, and this is presumably due to the extensive fluorination along the length of the molecule. Song *et al.*[31] reassigned the phase sequence of compound **25.3** (previously listed as only exhibiting the conventional nematic and ferroelectric nematic phases) and reported that this material also exhibited a SmA$_F$ phase on cooling. This was particularly interesting since the other examples of materials possessing the SmA$_F$ phase described earlier had incorporated

ChemPlusChem

Review

doi.org/10.1002/cplu.202300726

Chemistry Europe
European Chemical
Societies Publishing

fewer lateral fluorines in a DIO based structure. Adding exclusively the extra fluorine saw T_{NFN} increase by 55 °C, compared to the value reported by Li *et al.*[19] for compound **7**, but some 110 °C higher than the value reported by Matsukizono *et al.*[45] When the fluorine *meta* to the ester of DIO is replaced by a CF$_3$ group but the terminal cyano group is maintained, as seen in compound **26.3**, T_{NFI} increased by only 22 °C compared to DIO. This much smaller increase in transition temperature seen for compound **26.3** compared to **25.3** can presumably be attributed to the much larger lateral bulk endowed by the CF$_3$ group and the removal of the other *meta* fluorine. For compound **27** with a terminal CF$_3$ group, the increase in T_{NFN} compared to DIO is 69 °C and to compound **5** is 30 °C, and this suggests that having highly fluorinated biphenyl moieties capped by a polar group is particularly favourably for observing the N$_F$ phase. Taking compound **26.3** and exchanging the CF$_3$ group for a nitro group in the *meta* position to the ester as shown by compound **28.3**, sees T_{NFN} increase by 57 °C compared to DIO and by 40 °C compared to compound **26.3** even with the bulk of the nitro group being present. Comparing DIO and compound **22.3** there was a decrease of 3 °C with the addition of a lateral nitro group, which suggested that this lateral moiety was not optimal for enhancing the stability of the N$_F$ phase overall. However, the inclusion of the terminal cyano group in the case of compound **26** and the temperature trend seen, suggests that the interactions present in the formation of the N$_F$ phase are rather complex. Li *et al.*[19] also reported compound **29** where the ester linker is replaced by a difluoromethyl ether linker, a feature associated with another archetypal compound, namely UUQU-4N which will be discussed in greater detail later in the review. This material when compared to compound **25.3**, which is the corresponding material with an ester linker, sees T_{NFN} drop by 80 °C and a reduction in the average molecular dipole of 0.7 D. Li *et al.*[18] had also previously reported a set of DIO based materials with a methyl terminal and which contained this difluoromethyl ether linker as shown by compounds **30–32**. Compounds **30** and **31** have structures which contain both an ester linker and a difluoromethyl ether linker. While all three compounds show a range of different aromatic arrangements at the ether link, in all of these materials the N$_F$ phase is extinguished. Li *et al.*[19] also reported a further set of materials with a difluoromethyl ether linker with differing lateral and terminal groups attached to the aromatic rings. The N$_F$ phase in compounds **33–37** was completely destabilised, even in the cases when the dioxane ring was joined to a shorter terminal chain. This would appear indicative that the difluoromethyl ether linker has a destabilising effect on the formation of the N$_F$ phase.

The previous examples related to DIO have all had three aromatic rings incorporated into the molecular backbone, in Table 6 materials with only two aromatic rings are shown.[18,48] None of these compounds exhibit the N$_F$ phase, regardless of the composition of the substituents on the aromatic rings. Clearly removing one aromatic ring reduces the shape anisotropy of these materials compared to the compounds with three rings, a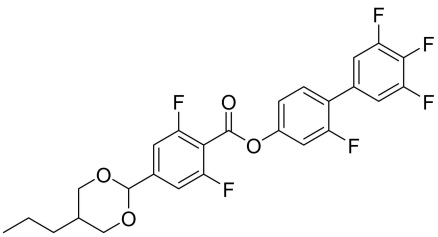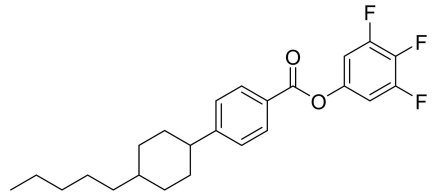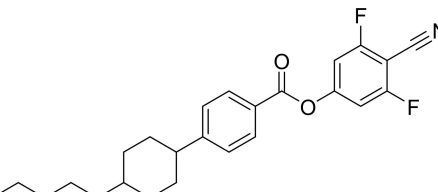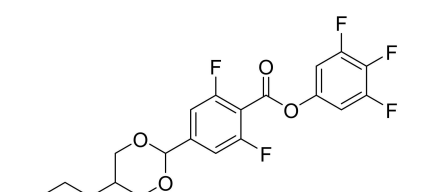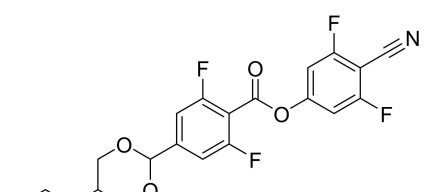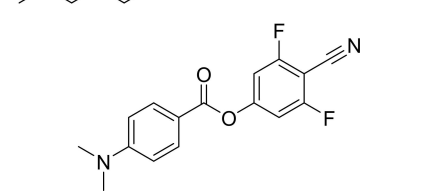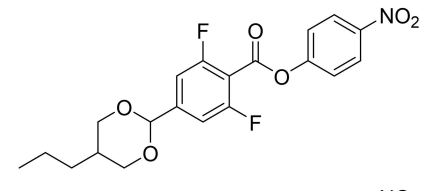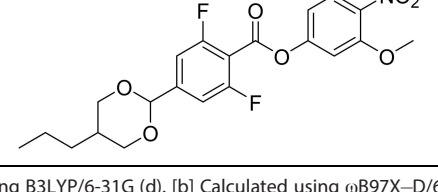s well as reducing the intermolecular interactions between the mesogenic units, and hence the liquid crystalline phase behaviour is suppressed.

When summarising the effect different modifications have on the stability of the N$_F$ phase for the materials based on DIO a few general trends become apparent. Shortening the length of the terminal carbon chain connected to the dioxane ring promotes the stability of the N$_F$ phase, while extending its length does the opposite and such an effect can be rationalised using the model proposed for the N$_F$ phase by Madhusudana.[52] Additional lateral fluorination in the aromatic ring of the biphenyl moiety connected to the ester, also appears to enhance the stability of the N$_F$ phase. Within Madhusudana's model, the addition of the fluorine atom increases the amplitude of the charge density on the associated aromatic ring and in relative terms decreases that associated with the terminal rings. Such a change is predicted to increase the stability of the N$_F$ phase. Removing any of the fluorines in the DIO system appears to be favourable for the formation of the SmA$_F$ phase by removing lateral bulk which helps to promote the interactions between the mesogenic units which is favourable for more ordered phases. Replacing lateral fluorine atoms with more bulky polar lateral substituents such as CF$_3$ and NO$_2$ saw a slight decrease in the N$_F$ transition temperatures. Replacing one of these fluorines with a methoxy group saw the N$_F$ phase again slightly destabilised and further lengthening this alkyloxy chain saw the phase be extinguished. However, replacing the central terminal fluorine for a CF$_3$, NO$_2$ or CN group (if the value reported by Li *et al.*[19] is used) seems to stabilise the formation of the N$_F$ phase. This is presumably due to the enhancement in the strength of the dipole in the terminal ring in combination with the fluorines *ortho* to the terminal group spreading the negative charge of the terminal group as well as preventing unfavourable anti–parallel correlations. Most of the other modifications that were made to the archetypal DIO structure had a negative impact on the N$_F$ transition temperatures highlighting the challenge in the molecular design of these compounds. Therefore, the stability of the N$_F$ phase in these DIO-based materials was based on the combination of changes made to the structure and if shape or electronic effects were more dominant. Indeed, this is shown by the relative stabilities of the N$_F$ and N phases being governed by a subtle interplay of steric and electronic factors, and this will be exemplified in the future discussions around the other archetypal N$_F$ materials.

3. Materials Based on UUQU-4N

UUQU-4N is the second archetypal ferronematogen that will be discussed. This family of materials reported in the literature, is currently far smaller in scale than both the DIO and RM734 families. UUQU-4N was a particularly exciting compound when it was reported in 2021 by Manabe *et al.*[24] as it exhibits the N$_F$ phase at around room temperature but without the very high melting points described elsewhere. UUQU-4N is characterised by having at one terminus an alkyl chain linked to a fluorinated biphenyl, and at the other a 2,6-difluorocyanophenyl. The two

Table 6. The molecular structures, phase sequences and average dipole moments of compounds **38–44**.

Compound	Structure	Melting Point/°C	Phase Sequence/°C	ΔT_{NF}/°C	μ/D	Ref.
1		96	I–174–N–85–N_X–69–N_F–34–Cr	–	9.4[a]	7,21
38		91	I–98–N	×	6.4[b]	48
39		79	I–151–N	×	9.2[b]	48
40		68	I–16–Cr	×	8.5[b]	48
41		83	I–93–N–54–Sm	×	12.1[b]	48
42		165	I–148–Cr	×	11.8[b]	48
43		–	I–67–Cr	×	10.2[c]	18
44		–	I–24–N	×	10.4[c]	18

[a] Calculated using B3LYP/6-31G (d). [b] Calculated using ωB97X–D/6-311G (d,p). [c] Calculated using B3LYP/6-311+G(d,p).

termini are linked by a difluoromethyl ether group, and this group was described earlier in relation to some of the compounds based on the DIO structure. However, despite usually not containing an ester like DIO, the extensive fluorination of the molecules provided a suitably large longitudinal molecular dipole, which was calculated to be 11.3 D,[24] and allowing the N_F phase to form. UUQU-4N is labelled compound **45** and shows a phase sequence on cooling of I-19.6 °C—N_F and this will be used as the representative temperature the rest of the materials will be compared to. The effect of making modifications to the UUQU-4N structure and how that changes the stability of the N_F phase is shown in Table 7.[9,53,54] Nishikawa et al.[51] reported that reducing the length of the terminal alkyl chain and replacing the difluoromethyl ether linker with an ester, as seen in compounds **46.2** and **46.3**, saw the N_F phase stabilised dramatically compared to compound **45**. The stabilisation of the N_F phase when the terminal alkyl chain is short is supported by T_{NFI} increasing by 25 °C when the propyl chain in compound **46.3** is reduced to an ethyl chain in compound **46.2**. Chen et al.[53] reported compound **47.2**, which has an ethyl terminal chain sees the N_F phase stabilised by just under 50 °C compared to the parent compound. Interestingly, the phase sequence is also completely changed with the N_F phase preceded by the N_X phase and the conventional nematic phase. This suggests, however, that the terminal oxane ring is more favourable for stabilising the N_F phase than just the butyl chain on its own. Chen et al.[53] also reported compound **47.7** with a heptyl terminal chain but in this case the N_F phase was completely destabilised with only the conventional nematic and N_X phases present. This observation is in good agreement with the effect that the terminal chain had on the stability of the N_F phase for the materials based on the DIO structure i.e., that increasing the terminal chain length destabilised the N_F phase. Compound **47.3** with the same structure as compounds **47.2** and **47.7** but with a propyl terminal chain was reported by Kirsch et al.[54] but this report preceded the experimental discovery of the N_F phase. The smectic C phase reported for compound **47.3** may in fact be the N_X phase described earlier, since this compound was reported in 2008 prior to the reports of the N_F and N_X phases, and so if the N_F phase was present, it would be at a lower temperature than this and therefore has been destabilised compared to compound **47.2**. They also reported compound **48** where the terminal cyano group was replaced by a fluorine, and there was a clear decrease in T_{NI} compared to compound **47.3** but there was no mention of a phase change which could be potentially assigned as the N_F phase. Kirsch et al.[54] additionally described compounds **49** and **50** where the terminal fluorinated phenyl was replaced by a fluorinated biphenyl which is a feature more commonly seen with DIO. These materials again appeared to have the N_F phase absent, however, it must again be stressed that their report predates that of the N_F phase. The structures do appear to have the characteristics that would allow for the observation of the N_F phase. Li et al.[19] reported compound **51** in which the difluoromethyl ether linker was replaced by an ester linker and the terminal 2,6-difluorocyanophenyl replaced

by a nitrophenyl moiety and this material did not show the N_F phase.

Unlike with DIO there has not been such an extensive variety of modifications to the UUQU-4N structure reported in the literature to date. However, there are still some general observations that can be made on the stability of the N_F phase with regards to these structures. Replacing the terminal alkyl chain by an alkyl terminated oxane ring appears to stabilise the N_F phase compared to UUQU-4N, presumably due to a change in electron density associated with the fluorinated biphenyl moiety. Much like with the DIO–based compounds, extending the terminal alkyl length connected to the oxane ring reduces the stability of the N_F phase and when the chain is long enough the N_F phase is completely suppressed.

4. Materials Based on RM734

RM734, as the introduction described was the first material to be proven to exhibit the ferroelectric nematic phase and its family contains the largest number of compounds of the three N_F archetypes. RM734 has a structure characterised by a three ring system connected by ester linkers with a nitro group at one terminus and two alkyloxy groups at the other and this gives the molecule its very large average dipole moment, calculated to be 11.4 D.[6,8,21] RM734, much like DIO, showed a large polarisation value of around 6 μC cm^{-2}.[8] RM734, labelled compound **52**, shows a phase sequence on cooling of I–188 °C–N-133 °C–N_F and will be used as the baseline N_F transition temperature that the other materials in this family will be compared to. While RM734 was not the first material in this family to show a nematic-to-nematic phase transition as strictly that was RM230 (compound **53.2**),[5] RM734 has been the most extensively studied. The first set of tables will look to study small modifications to the RM734 molecular structure, and these will increase in complexity later in this review. Table 8 looks at the effect of changing the length of the terminal alkyloxy chain and Mandle et al.[6] reported that as the chain increased in length, the stability of the N_F phase diminished until it was completely lost. Increasing the terminal methoxy to an ethoxy saw T_{NFN} decrease by around 50 °C and for propoxy the phase was not seen in the compound's neat state but only as a virtual transition temperature, such that T_{NFN} would have been some 125 °C lower than RM734. The destabilisation of the N_F phase can again related to the model of the N_F phase posed by Madhusudana since increasing the terminal chain length will increase electron density within that terminal aromatic ring which is unfavourable for the N_F phase.[52] Table 8 also shows compounds **54** and **55** which have a diether terminal chain and these were reported by Li et al.[18] Much like the other compounds with longer terminal chain lengths, this material did not exhibit the N_F phase.

There were also changes made to the extent of fluorination on the backbone of the RM734 molecule at a variety of positions, and these are summarised in Table 9. Mandle et al.[6] reported that introducing a fluorine ortho to the terminal nitro group of RM734 increased the longitudinal dipole moment to

Table 7. The molecular structure, phase sequence and average dipole moment of compounds 45–51.
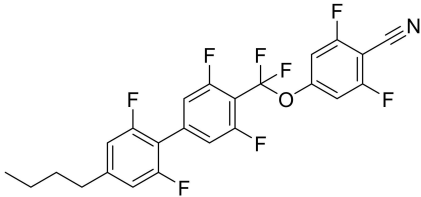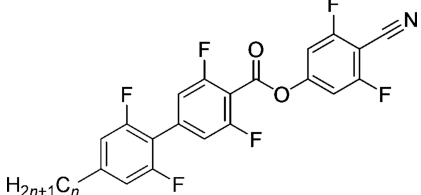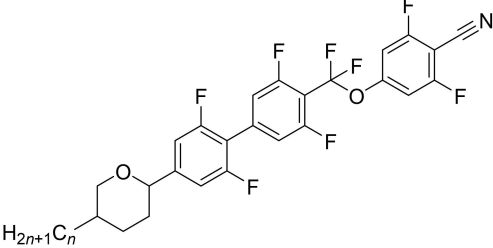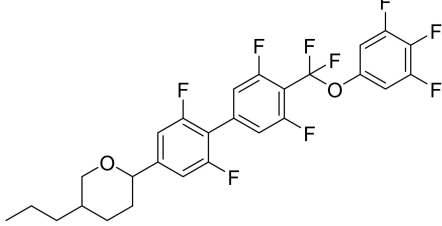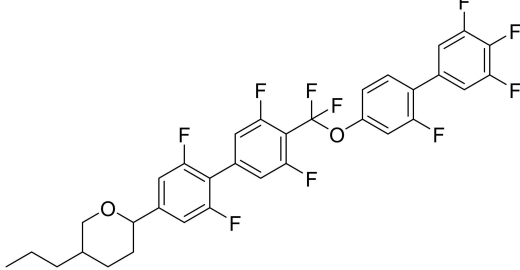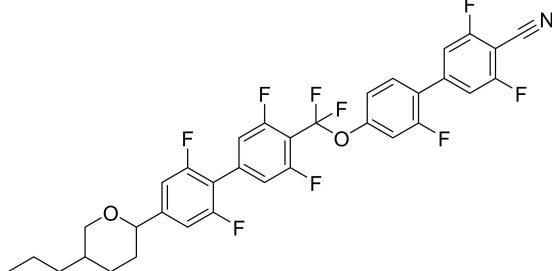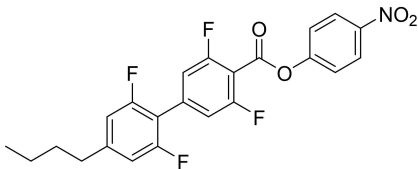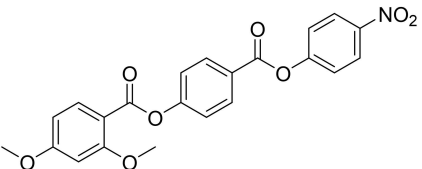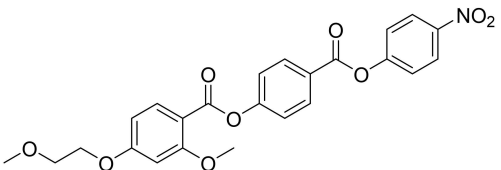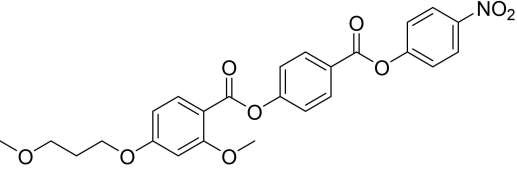
Compound		Structure	Melting Point/ °C	Phase Sequence/°C	ΔT_{NF}/ °C	μ/D	Ref.
45			96	I–20–N_F	–	11.3[a]	24
46	2		136	I–150–N_F–121–Cr	+130	12.6[b]	51
	3		104	I–125–N_F–69–Cr	+105	12.7[b]	51
47	2		–	I–128–N–83–N_X–69–N_F	+49	–	53
	3		74	I–144–N–67–SmC	×	–	54
	7		–	I–128–N–33–N_X	×	–	53
48			83	I–83–N	×	–	54
49			98	I–193–N	×	–	54
50			96	I–241–N	×	–	54

Table 7. continued

Compound	Structure	Melting Point/°C	Phase Sequence/°C	ΔT_{NF}/°C	μ/D	Ref.
51		–	I–95–N–68–Cr	×	11.0[b]	19

[a] Calculated using B3LYP/6-31G(d). [b] Calculated using B3LYP/6-311+G(d,p).
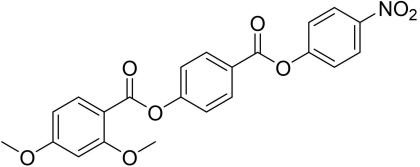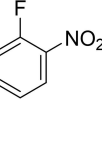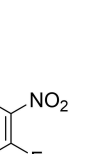
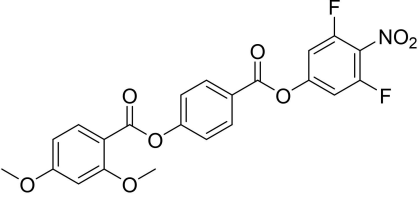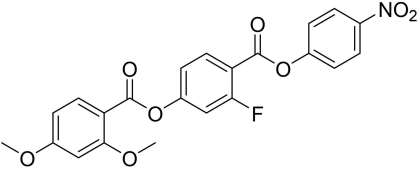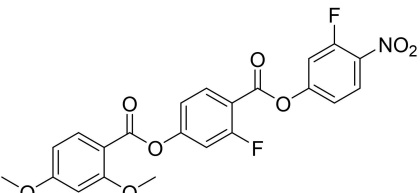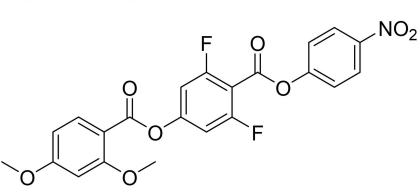12.1 D and T_{NFN} increased by 7 °C, despite the additional lateral bulk provided by the fluorine. The increase in the stability of the N_F phase associated with the addition of the fluorine atom may be attributed to changes in the molecular dipole moment and molecular polarizability but this can also be related to the model proposed by Madhusudana.[52] The parallel alignment of these rods is enhanced by reducing the amplitude of the charge density wave at either end of the molecule, including the nitro containing ring, and this was presumably achieved by the addition of the lateral fluorine substituent that removes electron density from the nitro group. The same modification to compound **53.2** to give compound **56.2** sees an even larger stabilisation of the N_F phase increasing it by 31 °C. However, in both cases there was a decrease in T_{NI} of around 32 °C indictive

of the decrease in shape anisotropy caused by the addition of a lateral fluorine. Mandle[55] also reported that adding a second fluorine *ortho* to the terminal nitro group as seen in compound **57** stabilised the N_F phase by a further 8 °C compared to compound **56.1**. Furthermore, this addition saw the conventional nematic phase destabilised, and a direct N_F—I transition was observed. Brown *et al.*[21] reported that adding a fluorine instead to the middle aromatic ring, as seen in compound **58**, has a similar effect as adding it to the terminal ring, with the N_F phase seeing an increase in its transition temperature of 10 °C and this was supported by Li *et al.*[19] and Saha *et al.*, who also reported a spontaneous polarisation value of 6.9 cm^{-2} which is even higher than that found for RM734.[20] Saha *et al.*[20] also reported that this material exhibited multiple

Table 8. The molecular structure, phase sequence and average dipole moment of compounds **50–53**.

Compound		Structure	Melting Point/°C	Phase Sequence/°C	ΔT_{NF}/°C	μ/D	Ref.
52			140	I–188–N–133–N_F	–	11.4[a]	6,8
53	2		139	I–182–N–86–N_F	−47	11.7[a]	5,6
	3		135	I–161–N	×	–	6
	4		111	I–160–N	×	–	6
	5		99	I–150–N	×	–	6
	6		110	I–149–N	×	–	6
54			–	I–152–N–117–Cr	×	9.6[b]	18
55			–	I–128–N	×	12.3[b]	18

[a] Calculated using B3LYP/6-31G (d). [b] Calculated using B3LYP/6-311+G(d,p).

Table 9. The molecular structures, phase sequences and average dipole moments of compounds **56–60**.

Compound		Structure	Melting Point/°C	Phase Sequence/°C	ΔT_{NF}/°C	μ/D	Ref.
52			140	I–188–N–133–N_F	–	11.4[a]	6,8
56	1		165	I–155–N–140–N_F	+7	12.1[a]	6
	2		142	I–150–N–117–N_F	−16	12.5[a]	6
57			174	I–148–N_F	+15	–	55
58			161	I–165–N–143–N_F	+10	12.0[a]	19–21
59			151	I–139–N_F	+6	13.1[a]	21,55
60			–	I–141–N_F–121–Cr	+8	13.0[b]	19

[a] Calculated using B3LYP/6-31G (d). [b] Calculated using B3LYP/6-311+G(d,p).

ferroelectric nematic phases and not just the single polar phase described elsewhere. Adding a second lateral fluorine to compound **58**, *ortho* to the terminal nitro group to give compound **59**, did lead to the N_F phase still being stabilised compared to RM734, and exhibiting a direct N_F–I transition. However, there was a slight decrease in the N_F transition temperature compared to the two materials that only had a single lateral fluorine substituent. Li *et al.*[19] also described compound **60** which had a second fluorine substituent on the middle aromatic ring and much like compound **59**, showed a stabilisation of the N_F phase compared to RM734 but T_{NFI} was lower than that found for the singly substituted material, compound **58**.

The influence of increasing the lateral alkyloxy chain length in the terminal aromatic ring is described in Table 10. Pociecha *et al.*,[14] Li *et al.*[18] and Cruickshank *et al.*[37] have all reported on the effect of extending the lateral alkyloxy chain length of RM734 in series **61**. T_{NFN} decreases with the increase of the lateral chain length, albeit less quickly than that seen for increasing the terminal alkyloxy chain length, until it reaches a limiting value when $m = 6$, Figure 6. Weissflog and Demus[56,57] reported a similar trend for conventional low molar mass mesogens which contained a lateral alkyl chain and suggested that the trend seen was because the lateral alkyl chain adopted conformations in which it lay parallel to the molecular axis, Figure 7. The decrease in the stability of the N_F phase can

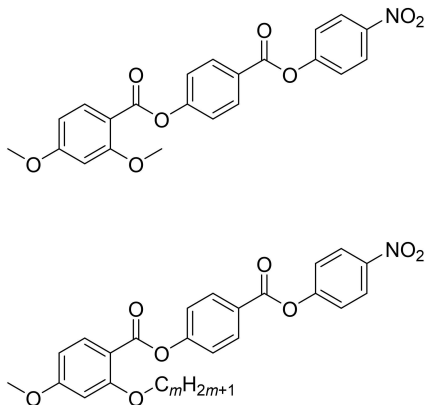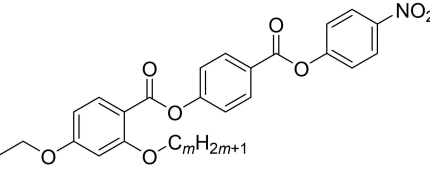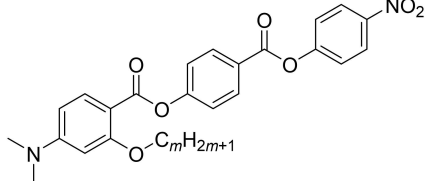**Table 10.** The molecular structures, phase sequences and average dipole moments of compounds **61–67**.
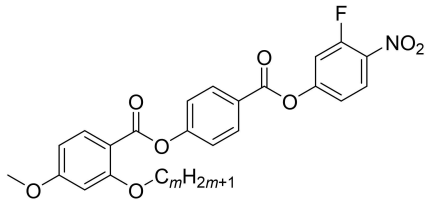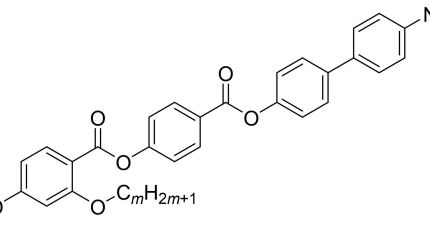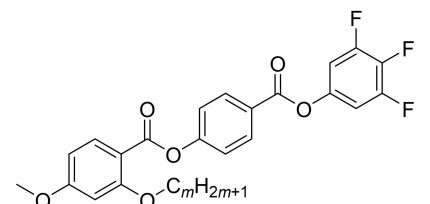
Compound		Structure	Melting Point/°C	Phase Sequence/°C	ΔT_{NF}/°C	μ/D	Ref.
			140	I–188–N–133–N_F	–	11.4[a]	6,8
61	2		159	I–131–N–106–N_F	−27	11.2[a]	14,37
	3		147	I–97–N–85–N_F	−48	11.2[a]	14,18,37
	4		141	I–75–N–65–N_F	−68	11.2[a]	14,37
	5		132	I–61–N–54–N_F	−79	11.2[a]	14,18,37
	6		101	I–50–N–44–N_F	−89	11.2[a]	14,37
	7		110	I–50–N–44–N_F	−89	11.2[a]	37
	8		123	I–51–N–44–N_F	−89	11.2[a]	37
	9		117	I–49–N–42–N_F	−91	11.2[a]	37
62	2		143	I–143–N–91–N_F	−42	–	6
	3		143	I–143–N–78–N_F	−55	–	6
63	1		188	I–170–N_F	+37	≈14	58
	2		150	I–136–N_F	+3	≈14	58
	3		156	I–116–N_F	−17	≈14	58
	4		144	I–96–N_F	−37	≈14	58
	5		120	I–82–N_F	−51	≈14	58
	6		104	I–65–N_F	−68	≈14	58
64	2		161	I–109–N_F	−27	12.2[a]	37
	3		129	I–88–N_F	−48	12.2[a]	37
	4		119	I–69–N_F	−68	12.2[a]	37
	5		105	I–56–N_F	−79	12.2[a]	37
	6		77	I–48–N_F	−89	12.2[a]	14,37
	7		93	I–47–N_F	−89	12.1[a]	37
	8		111	I–48–N_F	−89	12.2[a]	37
	9		105	I-46-N_F	−91	12.1[a]	37
65	1		230	I–363–N–141–N_F[a]	+8	11.7[a]	42,55
	2		214	I–293–N–128–N_F	−5	≈12[a]	42
	3		195	I–259–N–111–N_F	−22	≈12[a]	42
	4		153	I–235–N–95–N_F	−38	≈12[a]	42
	5		156	I–218–N–82–N_F	−51	≈12[a]	42
	6		150	I–206–N–70–N_F	−63	≈12[a]	42
	7		164	I–199–N–69–N_F	−64	≈12[a]	42
	8		191	I–190–N–69–N_F	−64	≈12[a]	42
	9		188	I–181–N–65–N_F	−68	≈12[a]	42
66	1		–	I–78–Cr	×	9.0[b]	18
	2		–	I–97–Cr	×	8.9[b]	18
	3		–	I–101–Cr	×	8.9[b]	18
	4		–	I–11–N	×	8.9[b]	18
	5		–	I–16–N	×	8.9[b]	18

ChemPlusChem

Review
doi.org/10.1002/cplu.202300726

Chemistry Europe
European Chemical
Societies Publishing

Table 10. continued						
Compound	Structure	Melting Point/°C	Phase Sequence/°C	ΔT_{NF}/°C	μ/D	Ref.
67 1		173	I–200–N	×	11.6[a]	6,18
4		–	I–66–N–48–Cr	×	11.0[b]	18
[a] Calculated using B3LYP/6-31G (d). [b] Calculated using B3LYP/6-311+G(d,p).						

presumably be related to the reduction in structural anisotropy as the lateral chain length is increased and so when the chain becomes more parallel to the long molecular axis, as described by Weissflog and Demus, the destabilisation of the N_F phase is mitigated.

Mandle *et al.*[6] also reported that T_{NFN} decreased with increasing lateral chain length for series **62** which had an ethoxy terminal chain but at lower temperatures than seen for the equivalent methoxy terminated homologues. Cigl *et al.*[58] reported another series, series **63**, in which the lateral alkyloxy
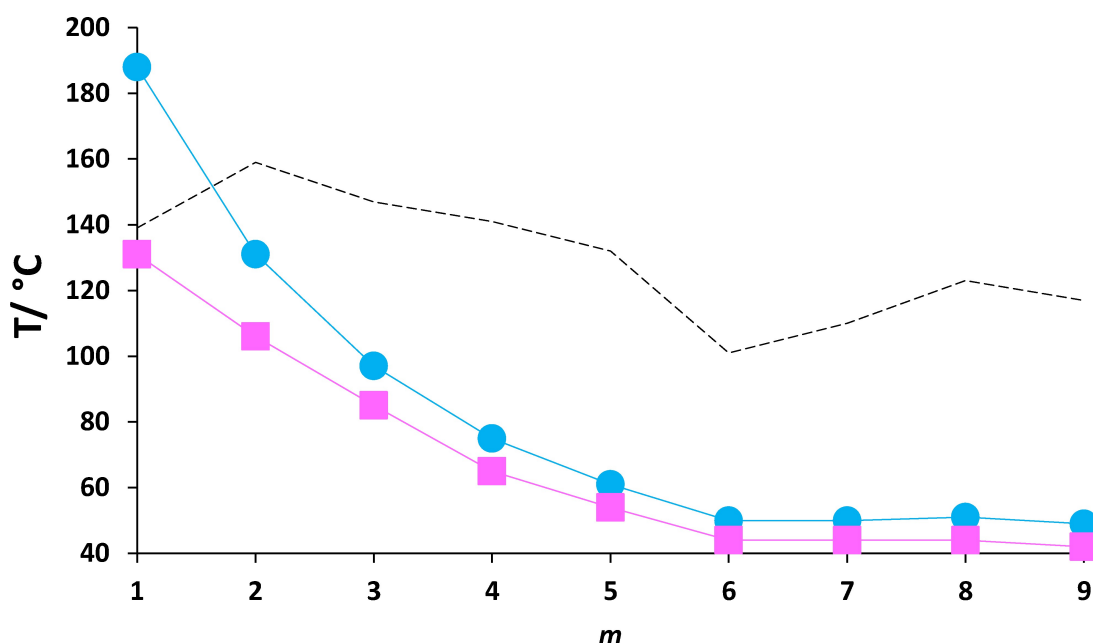

Figure 6. Dependence of the transition temperatures on the number of carbon atoms in the lateral alkyloxy chain, *m*, for series **61**, the values of T_{NI} are represented by filled circles, T_{NFN} by filled squares and the melting points are connected by the broken line with dashes.
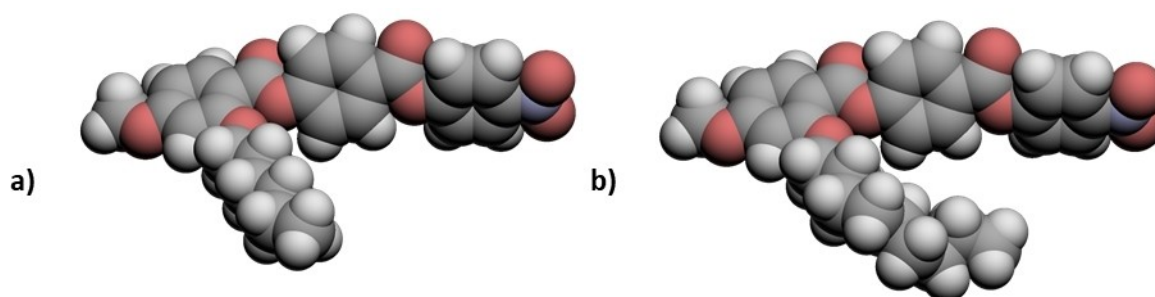

Figure 7. A comparison of the molecular shapes for members of series **61**: (a) compound **61.6** and (b) compound **61.9**. In (b) the lateral chain contains gauche linkages causing it to lie more along the molecular long axis, as similarly was described by Weissflog and Demus,[56,57] and the molecular breadth becomes insensitive to chain length. If the chain continued to extend in an all–trans manner as shown in (a) then the transition temperatures should continue to fall for compounds **61.7** to **61.9**.

ChemPlusChem

Review
doi.org/10.1002/cplu.202300726

**Chemistry
Europe**
European Chemical
Societies Publishing

chain length was extended but, in this case, the terminal methoxy group was replaced by a dimethylamino group. The N_F phase was stabilised by around 30°C compared to the values seen for series **61**, but on this occasion the transition seen was directly from the isotropic phase. Furthermore, these materials had molecular dipoles that were around 3 D higher than those calculated for series **61**. Compound **63.1** was also reported by Mandle[55] and the transition temperatures were in good agreement with those reported by Cigl et al. In Table 10, series **64**, reported by Pociecha et al.[14] and Cruickshank et al.[37] is described in which again the lateral alkyloxy chain is extended much like series **61** but here a fluorine is added ortho to the terminal nitro group much like some of the materials shown in Table 9. The temperature trend for series **64** was similar to that described for series **61** but with the N_F phase stabilised in comparison. The addition of the fluorine ortho to the nitro group did see T_{NI} be destabilised in this series due to the reduction of shape anisotropy and it therefore exhibited mostly direct N_F–I transitions. The members of series **64** have dipole moments 1 D larger than series **61**, similar to other material with the same modification. However, the increase in the N_F phase transition temperatures was attributed to the electronic distribution of the molecules and how that related to the model proposed by Madhusudana.[52] Cruickshank et al.[42] also made another modification to the terminal aromatic ring containing the nitro group by replacing it with a nitrobiphenyl moiety as shown by series **65** in Table 10. Having a four aromatic ring system saw T_{NI} increase dramatically, by over 150°C on average compared to series **61**, and presumably this increase may be attributed to the greater shape anisotropy introduced by the additional aromatic ring but also to the enhanced intermolecular interactions between the mesogenic units. The values of T_{NFN} were also higher than those seen for series **61**, however, this increase was only 24°C which is much smaller than the increase in stability seen for the conventional nematic phase. The longitudinal dipole moment of compound **65.1** is 11.7 D which is 0.31 D larger than RM734 and this is a small change considering the increase in the transition temperatures and again suggests that additional effects must be considered as the driving force for the formation of the N_F phase. The increase in T_{NFN} may be attributed to the change in the molecular shape with the addition of the extra aromatic ring and so the structural anisotropy is enhanced. The increase may also be explained by the additional ring spreading the charge distribution of the terminal moiety such that the amplitude at the molecular terminus is reduced and so following Madhusudana's model the N_F phase is stabilised.[52] Compound **65.1** was also reported by Mandle,[55] who observed a value of T_{NFN} around 20°C higher than that reported by Cruickshank et al.[42] Series **66** and **67** in which the terminal nitrophenyl moiety was replaced by a 3,4,5- trifluorophenyl moiety and a cyanophenyl moiety, respectively, were reported by Li et al.,[18] but none of the members of either series exhibited the N_F phase regardless of the length of the lateral alkyloxy chain. Compound **67.1** had been previously reported by Mandle et al.[6] and the transition temperatures were in good agreement. It was suggested by Mandle et al.[23] that although compound **67.1** and RM734 have

similar overall longitudinal molecular dipoles, compound **67.1** is unable to pack as efferently into the parallel orientation required for the N_F phase and presumably can instead form anti–parallel correlations.

The influence of changing the substituents on the terminal alkyloxy ring on the stability of the N_F phase is summarised in Table 11. Mandle et al.[6,47] reported compounds **68.2**, **69.2** and **70** in which the lateral alkyloxy chain of compound **53.2** was replaced by a hydrogen, hydroxy and methyl group, respectively and these materials all saw the N_F phase be completely destabilised and only a virtual transition temperature was reported. Compound **68.2** highlights the importance of having some degree of lateral bulk on the formation of the N_F phase, T_{NI} was around 80°C higher than RM734 due to the enhancement in shape anisotropy but the N_F phase was not observed. Li et al.[18] also reported that compound **68.2** did not exhibit the N_F phase. Unsurprisingly increasing the terminal chain length in both series **67** and **69**, as reported by Mandle et al,[47] did not allow for the N_F phase to be observed. Li et al.[18] replaced the lateral alkyloxy chain with a diether chain and both compounds **71** and **72** did not exhibit the N_F phase despite having a sufficiently large molecular dipole. When a racemic 2-methylbutoxy group was added laterally to replace the lateral methoxy group, to give compound **73** the N_F phase was destabilised by almost 80°C, as was reported by Szydlowska et al.[59]

As Table 11 shows, a chiral 2-methylbutoxy group can be added to the RM734 template, as described by Pociecha et al.[14] for compound **74**. The transition temperatures of compounds **73** and **74** were the same but the conventional nematic phase was replaced by a chiral nematic phase and the ferroelectric nematic phase by its chiral counterpart. The chiral ferroelectric nematic phase, also termed the helielectric nematic phase, possessed a helix with the opposite twist sense than the preceding chiral nematic phase and maintained a pitch which was a few microns in length. Zhao et al.,[60] also reported the same material but did not observe the N_F* phase in a pure sample but did in mixtures and they called the phase the helielectric nematic phase. Zhao et al.[60] also reported compounds **75**, **76** and **77**, again which had chiral 2-methylbutoxy groups added to the molecule, but these also did not exhibit the N_F* phase in any of the pure compounds. Adding a fluorine ortho to the terminal nitro group of compound **73** to give compound **78**, saw the chiral nematic phase extinguished and a direct N_F*–I transition observed instead. The N_F phase was at an identical temperature to compound **73**, however, T_{NFI} was still much lower than T_{NFN} of RM734.

The influence that changing the substituents has on the middle aromatic ring on the stability of the N_F phase is described in Table 12. Tufaha et al.[33] described the effect of having the lateral alkyloxy chain on the middle ring instead of the terminal ring with the methoxy group in series **79**. The temperature trend observed was similar to that found for series **61** with the value of T_{NFN} decreasing as the length of the lateral alkyloxy chain increased. Indeed, compound **79.1** is an isomer of RM734 but with the lateral methoxy being in the middle ring rather than the terminal aromatic ring and they

ChemPlusChem

Review
doi.org/10.1002/cplu.202300726

**Chemistry
Europe**
European Chemical
Societies Publishing

Table 11. The molecular structures, phase sequences and average dipole moments of compounds **68–78**.
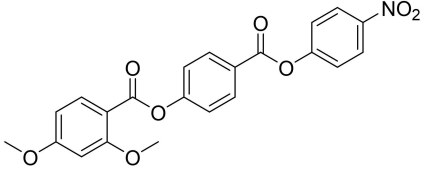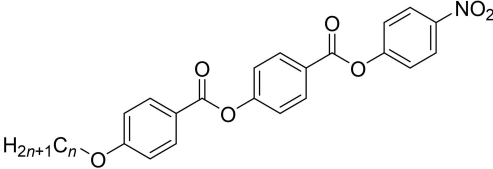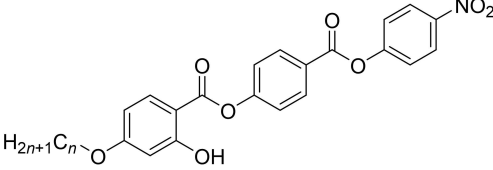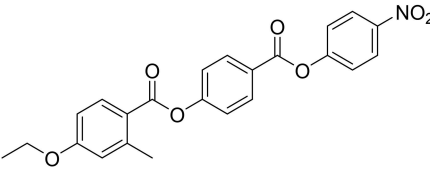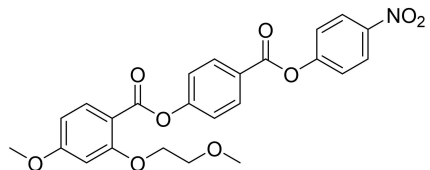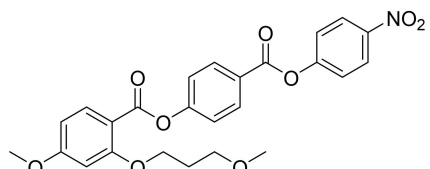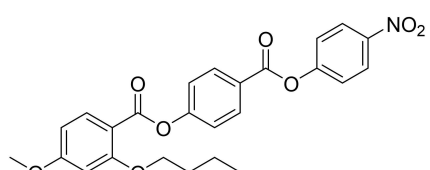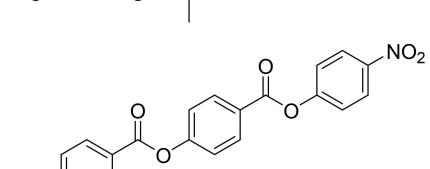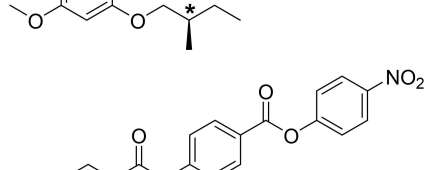
Compound		Structure	Melting Point/°C	Phase Sequence/°C	ΔT$_{NF}$/°C	μ/D	Ref.
52			140	I–188–N–133–N$_F$	–	11.4[a]	6,8
68	1		204	I–267–N	×	10.3[a]	47
	2		155	I–276–N	×	≈10[a]	6,47
	3		148	I–275–N	×	≈10[a]	47
69	1		210	I–240–N[a]	×	11.7[a]	47
	2		165	I–240–N[a]	×	≈12[a]	6,47
	3		137	I–240–N[a]	×	≈12[a]	47
70			139	I–186–N	×	–	6
71			–	I–152–N–117–Cr	×	12.2[b]	18
72			–	I–128–N	×	11.6[b]	18
73			141	I-56-N-55-N$_F$	−78	11.1[b]	59
74			140	I–56–N*–55–N$_F$*	−78	11.1[a]	14
75			138	I–42–N*	×	–	60

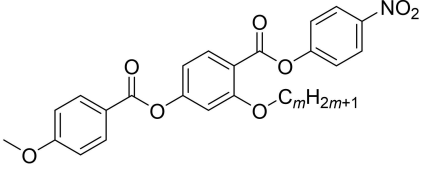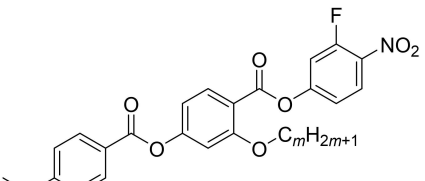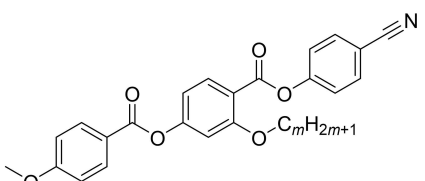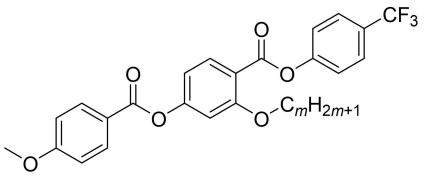| Table 11. continued						
Compound	Structure	Melting Point/°C	Phase Sequence/°C	ΔT_{NF}/°C	μ/D	Ref.
76		–	I–105–N*	×	–	60
77		–	I–67–N*	×	–	60
78		111	I–55–N_F*	−78	12.1[a]	14
[a] Calculated using B3LYP/6-31G (d). [b] Calculated using B3LYP/6-311+G(d,p).						
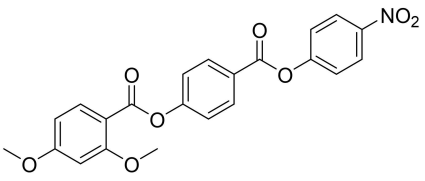
show similar transition temperatures. Series **79** had average dipole moments that were around 0.5 D larger than that of series **61**, the angle between the molecular axis and the molecular dipole was larger and on average showed higher values of T_{NFN}. Changing the position of the alkyloxy chain also changed the electronic distribution within the molecule such that the alkyloxy chain was no longer donating electrons to the terminal aromatic ring. This meant the amplitude of the charge density wave at the molecular terminus was reduced and this was favourable for the stability of the N_F phase in accord with the predictions of the model proposed by Madhusudana.[52] Li et al.[18] also reported **79.1**–**79.3**, with the transition temperatures for **79.1** being in good agreement, however there was a variance in the values of the other two compounds, with T_{NFN} of **79.2** = 97 °C and **79.3** = 105 °C. Tufaha et al.[33] also reported series **80** in which a fluorine was added ortho to the terminal nitro group and, much like was described earlier, in all members of the series the N_F phase was stabilised compared to series **79** and, except compound **82.1**, exhibited direct N_F–I transitions. The relative stabilisation of the N_F phase in this series can be justified much like series **65** using Madhusudana's model.[52] Li et al., reported series **81** and **82** in which the terminal nitro group was replaced by cyano and CF_3 groups, respectively. None of the members of either series exhibited the N_F phase.

The effect of other simple changes to the RM734 structure on the stability of the N_F phase is described in Table 13. Mandle[55] used a neural network in order to generate structures that might exhibit the N_F phase, suggesting that this method particularly favoured highly polarisable materials such as compounds **83** and **84**. Interestingly, while compound **83**

showed an enhancement in T_{NFNX} compared to RM734, compound **84** saw the N_F phase completely destabilised. Mandle et al.[6] had also previously reported other materials with large longitudinal dipole moments that did not appear to exhibit the N_F phase as shown by compounds **85**–**87**. Compound **86** not appearing to show the N_F phase was somewhat surprising considering a number of derivatives of this compound that will be described later do have the phase present, however, this may suggest that additional modifications are required to allow the molecules to pack effectively in a parallel manner. These observations also further highlighted that purely a large longitudinal dipole was not sufficient to observe the N_F phase. Mandle et al.[6] also reported compound **88** in which the terminal chain of compound **67.1** was extended from a methoxy to an ethoxy and again the N_F phase was not observed. Likewise, the N_F phase was extinguished when the direction of the ester linker attached to the terminal nitrophenyl moiety was reversed to give compound **89**. Mandle et al.[6] also reported that moving the lateral methoxy group of compound **53.2** from ortho to the ester to the meta position to give compound **90** was a further way to extinguish the N_F phase. This is presumably because the nitro group in this position will disrupt the ability of the molecules to pack together favourably to form the N_F phase. Mandle et al.[47] later described the effect of moving the position of the terminal nitro group from the para position to the meta position of the aromatic ring and found this lowered the dipole moment by 2 D as well as extinguishing the N_F phase. They also described the effect of moving the lateral hydroxy group of series **69** from the terminal aromatic ring with the alkyloxy chain to the middle aromatic

ChemPlusChem

Review
doi.org/10.1002/cplu.202300726

Chemistry
Europe
European Chemical
Societies Publishing

Table 12. The molecular structures, phase sequences and average dipole moments of compounds **79–82**.

Compound		Structure	Melting Point/°C	Phase Sequence/°C	ΔT_{NF}/°C	μ/D	Ref.
52			140	I–188–N–133–N$_F$	–	11.4[a]	6,8
79	1		192	I–189–N–126–N$_F$	−7	11.6[a]	18,33
	2		164	I–137–N–104–N$_F$	−29	11.6[a]	33
	3		130	I–105–N–93–N$_F$	−40	11.6[a]	33
	4		120	I–82–N–76–N$_F$	−57	11.6[a]	33
	5		102	I–66–N–61–N$_F$	−61	11.7[a]	33
	6		94	I–57–N–53–N$_F$	−80	11.7[a]	33
	7		72	I–54–N–51–N$_F$	−82	11.7[a]	33
80	1		180	I–156–N–141–N$_F$	+9	12.6[a]	33
	2		179	I–118–N$_F$	−15	12.6[a]	33
	3		135	I–92–N$_F$	−41	12.7[a]	33
	4		124	I–79–N$_F$	−54	12.8[a]	33
	5		104	I–68–N$_F$	−65	12.8[a]	33
	6		80	I–58–N$_F$	−75	12.8[a]	33
	7		73	I–55–N$_F$	−78	12.9[a]	33
81	1		–	I–186–N–140–Cr	×	10.5[b]	18
	2		–	I–134–N–92–Cr	×	10.3[b]	18
	3		–	I–94–N	×	10.3[b]	18
82	1		–	I–105–Cr	×	8.0[b]	18
	2		–	I–97–Cr	×	7.5[b]	18

[a] Calculated using B3LYP/6-31G (d). [b] Calculated using B3LYP/6-311＋G(d,p).

ring, series **92**, or the nitro containing terminal ring, series **93**, with none of the members of either series exhibiting the N$_F$ phase. Cruickshank *et al.* reported the evolution of phase behaviour from the N$_F$ phase to N$_X$ phase in RM734-type compounds for series **94** and **95**.[50] In both series as the terminal chain was increased in length the N$_F$ phase was destabilised to a greater extent than the N and N$_X$ phases and at longer chain lengths the N$_F$ phase was totally extinguished. Interestingly, series **95** with the alkyl terminal chain sees the N$_F$ and N$_X$ phases destabilised less than the equivalent members of series **94** which have an alkyloxy terminal chain. This was explained by the alkyloxy chain increasing the electron density at that terminal of the molecule and thus increasing the amplitude of the surface charge density wave which Madhusudana reported was unfavourable for the formation of the N$_F$ phase.[52] Cruickshank *et al.* also used series **95** to confirm the antiferroelectric structure of the N$_X$ phase which had been

similarly described previously by Chen *et al.*[49] Li *et al.*[18] reported that replacing either the terminal or lateral chain by a diether chain did not see the N$_F$ phase be observed, as was described previously. Replacing both chains with diether chains as seen in compound **96** did see the N$_F$ phase be exhibited, however, the phase was destabilised by 56 °C compared to RM734. They also reported in the same work that moving the lateral methoxy group in RM734 to *ortho* to the terminal nitro group as seen in compound **97.1** saw the N$_F$ phase no longer be observed. Li *et al.*[19] later reported that increasing the length of this lateral chain did not see the N$_F$ phase stabilised. This demonstrates that while it is important to have some degree of lateral bulk in these materials, the position of these groups is also key for the stability of the N$_F$ phase. In compound **98**, the lateral methoxy group is removed much like compound **68.1** but in this case the ester linker joining the nitrophenyl ring to the central aromatic ring is replaced by a methyl substituted

ChemPlusChem

Review
doi.org/10.1002/cplu.202300726

Chemistry Europe
European Chemical
Societies Publishing

Table 13. The molecular structures, phase sequences and average dipole moments of compounds **83–104**.
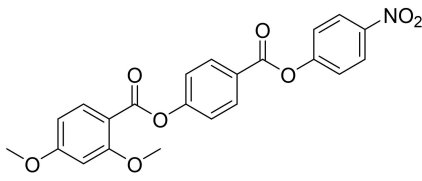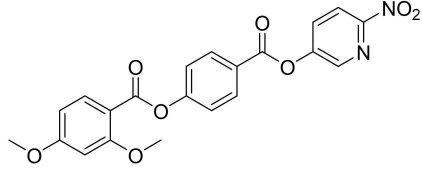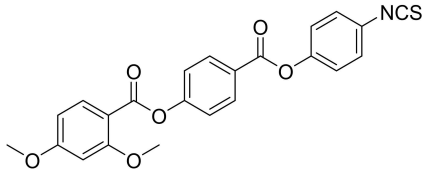
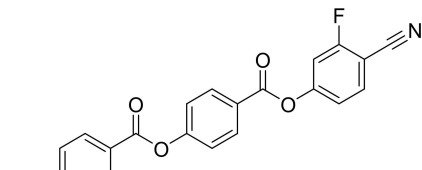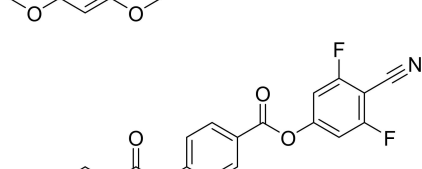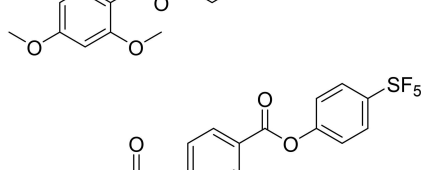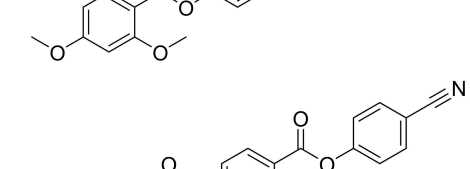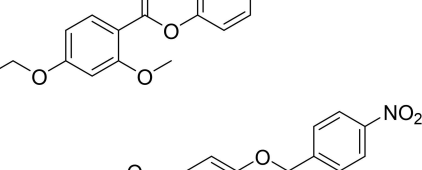| Compound	Structure	Melting Point/°C	Phase Sequence/°C	ΔT$_{NF}$/°C	μ/D	Ref.
52		140	I–188–N–133–N$_F$	–	11.4[a]	6,8
83		165	I–193–N–160–N$_X$–154–N$_F$	+21	–	55
84		153	I–163–N	×	–	55
85		173	I–170–N	×	12.0[a]	6
86		197	I–153–N	×	12.8[a]	6
87		163	I–93–N	×	10.5[a]	6
88		117	I–204–N	×	11.5[a]	6
89		181	I–190–N	×	8.3[a]	6
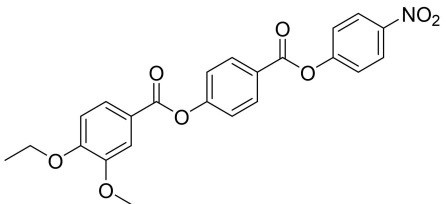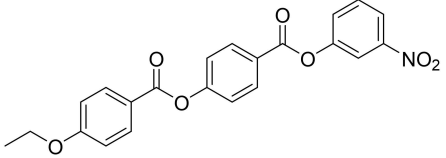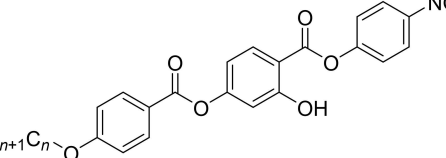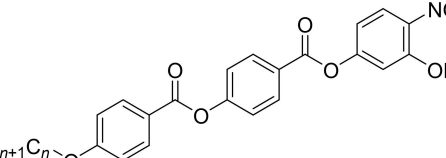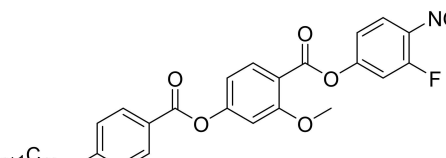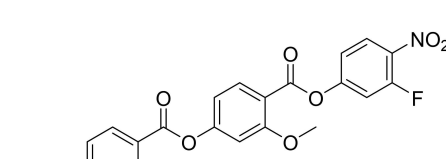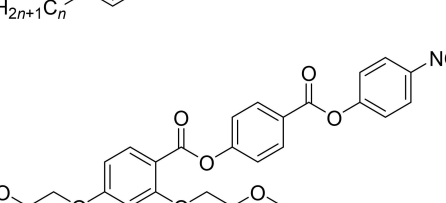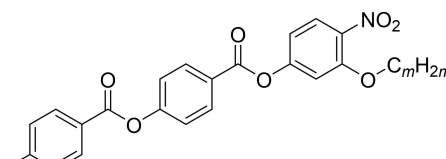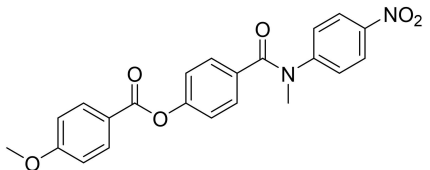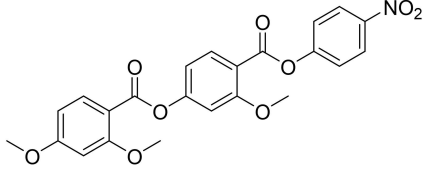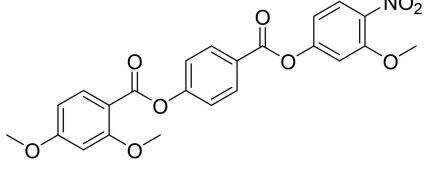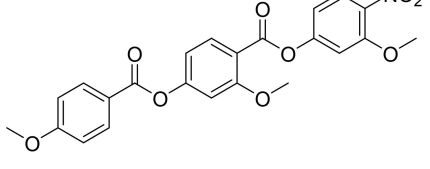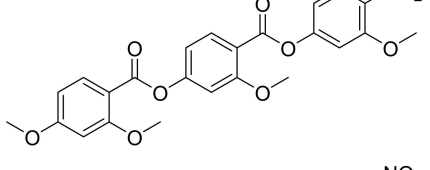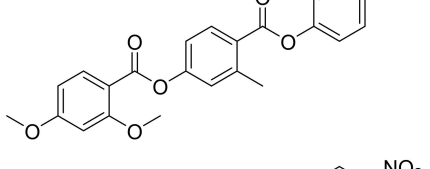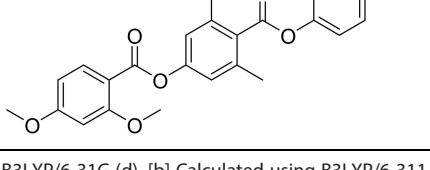
Table 13. continued

Compound		Structure	Melting Point/°C	Phase Sequence/°C	ΔT_{NF}/°C	μ/D	Ref.
90			172	I–182–N	×	–	6
91			160	Cr–160–I	×	9.4[a]	47
92	1		205	I–183–N	×	11.9[a]	47
	2		186	I–189–N	×	≈12[a]	47
	3		166	I–190–N	×	≈12[a]	47
93	1		163	I–155–N	×	11.6[a]	47
	2		150	I–180–N	×	≈12[a]	47
	3		137	I–197–N	×	≈12[a]	47.
94	1		179	I–157–N–142–N$_F$	+9	≈13[a]	50
	2		164	I–153–N–118–N$_X$–104–N$_F$	−29	≈13[a]	50
	3		145	I–133–N–79–N$_X$	×	≈13[a]	50
	4		128	I–130–N–38–N$_X$	×	≈13[a]	50
	5		92	I–118–N	×	≈13[a]	50
95	1		169	I–156–N$_F$	+23	≈12[a]	50
	2		146	I–132–N$_F$	−1	≈12[a]	50
	3		150	I–123–N–118–N$_X$–116–N$_F$	−17	≈12[a]	50
	4		120	I–105–N–92–N$_X$–79–N$_F$	−54	≈12[a]	50
	5		114	I–109–N–85–N$_X$	×	≈12[a]	50
	6		104	I–97–N–69–N$_X$	×	≈12[a]	50
96			–	I–119–N–76–N$_F$	−57	10.9[b]	18
97	1		–	I–162–Cr	×	9.3[b]	18
	2		–	I–127–Cr	×	10.6[b]	19
	3		–	I–112–Cr	×	10.7[b]	19

Table 13. continued

Compound	Structure	Melting Point/°C	Phase Sequence/°C	ΔT_{NF}/°C	μ/D	Ref.
98		–	I–106–Cr	×	4.5[b]	18
99		–	I–99–N_F	−34	12.2[b]	19
100		–	I–21–Cr	×	10.8[b]	19
101		–	I–120–Cr	×	12.3[b]	19
102		–	I–55–Cr	×	12.6[b]	19
103		–	I–108–N_F	−25	11.3[b]	19
104		150	Cr–150–I	×	10.7[b]	19

[a] Calculated using B3LYP/6-31G (d). [b] Calculated using B3LYP/6-311+G(d,p).

amide group. The molecular dipole calculated for compound **98** is almost 6 D smaller than compound **68.1**, there is presumably due to the conformation preference of the tertiary amide functionality,[61] and similarly does not show the N_F phase. The addition of a lateral methoxy group to the central aromatic ring of RM734 to give compound **99** as reported by Li *et al.*[19] saw the average molecular dipole increase by around 1 D and a direct N_F–I transition seen 34 °C below the value of T_{NFN} of RM734. The observation of a direct N_F–I transition can be attributed to the significant destabilisation of the convention nematic phase upon the addition of a second lateral methoxy group due to the decrease in structural anisotropy. The decrease seen in terms of the stability of the ferroelectric nematic phase is much smaller than that seen for T_{NI} and suggests that the conventional nematic phase is more sensitive to shape effects than the N_F phase. They also reported compounds **100** and **101** in which one of the lateral methoxy groups was instead substituted onto the terminal aromatic ring

ChemPlusChem

Review
doi.org/10.1002/cplu.202300726

Chemistry
Europe
European Chemical
Societies Publishing

ortho to the nitro group and in both these compounds the N_F phase was lost much like was seen for compound **97.1**. Li *et al.*[19] also reported that having a lateral methoxy group on all three of the aromatic rings was not conducive for the observation of the N_F phase as seen for compound **102**. Replacing the methoxy group attached to the middle ring of compound **99** by a methyl group to give compound **103**, the direct transition between the N_F phase and isotropic phase was maintained. The value of T_{NFI} for compound **103** was higher than compound **99** but was less than RM734, and this presumably was related to both the volume of the lateral substituents as well as their electronic properties. Li *et al.*[19] also reported that then adding a second lateral methyl group as seen in compound **104** has a destabilising effect on the N_F phase such that it was no longer observed. Since compound **60** showed the N_F phase despite two lateral groups substituted into the middle ring, there is therefore a suggestion that electron withdrawing groups are more favourable substituents in this ring for the stabilisation of the N_F phase than electron donating groups.

In Table 14 more complex changes are made to the RM734 structure while maintaining the terminal nitro group. Li *et al.*[18] reported that exchanging the ester linker joining the middle and terminal nitrophenyl aromatic rings with an azo moiety, regardless of the lateral substituents involved, saw the N_F phase extinguished. Li *et al.*[19] later reported a wide range of materials which often possessed additional lateral fluorination compared to RM734 as well as other modifications. Compound **108** had a structure much like compound **99** but with the lateral methoxy group in the terminal ring replaced by a fluorine substituent. The N_F phase is stabilised compared to RM734, despite the decrease in shape anisotropy associated with the fluorine. This was presumably because the fluorine is electron withdrawing and so it decreases the magnitude of the charge density wave associated with the molecule, in the terminal aromatic ring with the methoxy group, and thus stabilises the N_F phase according to Madhusudana's model. Li *et al.*[19] also reported that compound **109**, which had a second fluorine atom *ortho* to the ester group showed a stabilisation of the N_F phase. The additional fluorine destabilised the nematic phase as has been described earlier and so the material exhibited a direct N_F–I transition which was 2 °C higher than the value of T_{NFN} seen for compound **108**. They also described compound **110** in which the methoxy group in the middle ring was replaced by a CF_3 group. There was a large decrease in the N_F transition temperature both compared to RM734 being 41 °C lower. Interestingly, while compound **109** exhibited a direct N_F–I transition the addition of the CF_3 group saw the N_F phase destabilised compared to the conventional nematic phase which had remerged. This suggests that the CF_3 group decreases the shape anisotropy of the molecules and, in this position, is relatively unfavourable in terms of allowing the molecules to pack together in a parallel manner and hence the N_F phase is more strongly destabilised than the nematic phase. Taking compound **110** and removing one of the fluorines *ortho* to the ester group as seen in compound **111** saw the N_F phase completely destabilised despite having a similar dipole moment to

compound **110**. Li *et al.*[19] also reported compound **112** which had a structure similar to compound **111** but with the terminal methoxy group replaced by a methyl group and the lateral CF_3 group in the middle ring replaced by a fluorine. This material showed a dramatic stabilisation of the N_F phase having a value of T_{NFI} some 96 °C higher than that of RM734 and almost matches the very high N_F transition temperature observed for compound **25.1**. In compound **112**, the length of the terminal chain was reduced by removing the oxygen linking group and by having a single fluorine in both the terminal ring containing the methyl group and the middle ring. The increase in the stability of the N_F phase suggests that the ability of the molecules to pack together in a parallel orientation has been greatly enhanced. Compound **113** sees the lateral methoxy group in the terminal ring of compound **60** replaced by a CF_3 group while the high degree of fluorination in the middle ring was maintained. This compound also essentially has an exchange of the lateral groups between the methoxy terminal ring and middle aromatic ring. Again, much like was observed for compound **110**, the value of T_{NFN} sees a large decrease compared to RM734 with the inclusion of a lateral CF_3 group. Li *et al.*[19] described compound **114** which is a member of the RM734 family with no terminal chain. This compound did have three lateral fluorine substituents and interestingly showed a direct N_F–I transition which had been stabilised by 48 °C compared to the value of T_{NFN} for RM734. This suggests that a terminal chain is not a fundamental requirement to observe the N_F phase unlike what was found for the compounds based on DIO. Again, as has been highlighted previously compound **114** has a smaller average dipole moment than RM734 by some 0.9 D and so evidently there is not a direct link between the magnitude of the dipole moment and temperature at which the N_F phase is observed. Adding lateral bulk to the molecule as seen in compound **115** leads to a destabilisation of the N_F phase, this is despite one of the lateral groups being very polar in the form of the NO_2 group. As was described earlier these observations suggest that increasing the degree of fluorination for the aromatic rings is favourable for the formation of the N_F phase while bulky lateral groups destabilise the phase.

In Table 15, a set of materials are described in which the ester connected to the terminal nitro ring is removed to give a biphenyl moiety. As both Cruickshank *et al.*[42] and Mandle *et al.*[6,47] have described, removing this ester linking group sees the complete loss of N_F phase behaviour regardless of any other structural modifications made to the compounds. This included compound **128** in which two RM734 style molecules were joined together as a dimer by an alkyl spacer. Evidently the esters act to separate the regions of electron density within the molecule and so are important for allowing them to pack in a parallel orientation and thus the removal of the group sees the N_F phase completely destabilised.

The effect of multiple more complex changes to the RM734 structure, including the nature of the terminal polar group, on the stability of the N_F phase are summarised in Table 16. Li *et al.*[19] reported a wide array of materials which had the terminal nitrophenyl moiety replaced by a difluorocyanophenyl moiety and which are directly comparable to the nitrophenyl

ChemPlusChem

Review
doi.org/10.1002/cplu.202300726

Chemistry
Europe
European Chemical
Societies Publishing

Table 14. The molecular structures, phase sequences and average dipole moments of compounds **105–115**.
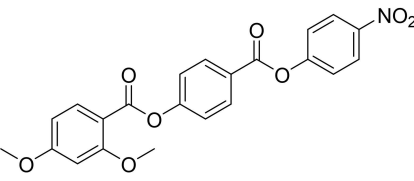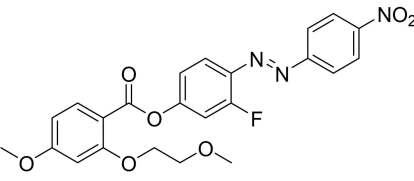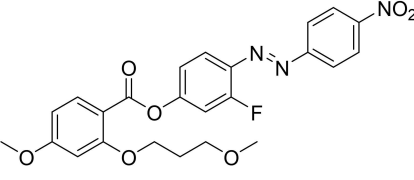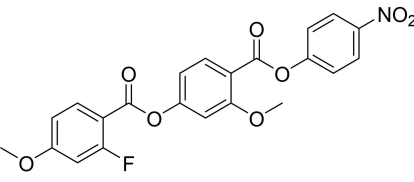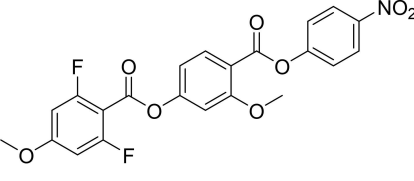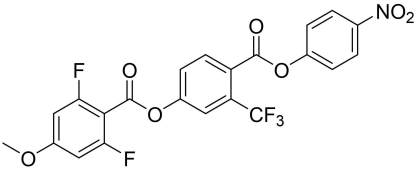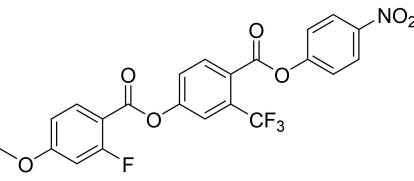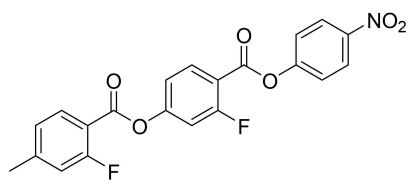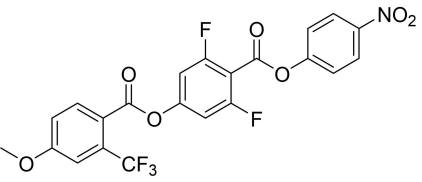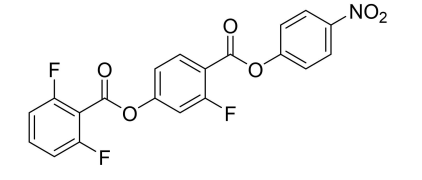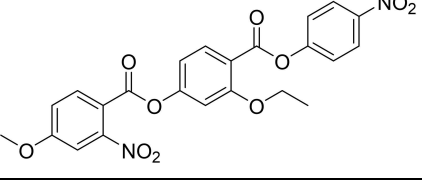
Compound		Structure	Melting Point/°C	Phase Sequence/°C	ΔT_{NF}/°C	μ/D	Ref.
52			140	I–188–N–133–N_F	–	11.4[a]	6,8
105	1		–	I–209–N–156–Cr	×	11.3[b]	18
	3		–	I–108–Cr	×	10.7[b]	18
106			–	I–117–Cr	×	11.6[b]	18
107			–	I–54–N	×	11.6[b]	18
108			–	I–178–N–158–N_F–150–Cr	+25	12.8[b]	19
109			–	I–160–N_F–112–Ce	+27	12.6[b]	19
110			–	I–115–N–92–N_F–75–Cr	−41	12.4[b]	19
111			-	I–129–N–63–Cr	×	12.5[b]	19
112			–	I–229–N_F–137–Cr	+96	11.5[b]	19

ChemPlusChem

Review
doi.org/10.1002/cplu.202300726

Chemistry Europe
European Chemical
Societies Publishing

Table 14. continued

Compound	Structure	Melting Point/°C	Phase Sequence/°C	ΔT_{NF}/°C	µ/D	Ref.
113		–	I–103–N–71–N_F–50–Cr	−62	12.4[b]	19
114		–	I–181–N_F–121–Cr	+48	10.5[b]	19
115		–	I–63–N_F	−70	12.3[b]	19

[a] Calculated using B3LYP/6-31G (d). [b] Calculated using B3LYP/6-311 + G(d,p).

homologues. As was demonstrated by the DIO and UUQU-4N compounds, the difluorocyanophenyl moiety is one which is favourable for observing the N_F phase. Compound **129** can be compared to compound **60** in terms of changing the terminal functionality of the molecule and the value of T_{NFI} increased by 21 °C with the inclusion of the difluorocyanophenyl moiety. The effect of the addition of this terminal group on the stability of the N_F phase is not independent of the other functionality within the molecule as shown by compounds **130** and **131**, but the replacement of the nitrophenyl moiety does generate a large increase in the average dipole moment. Compound **130** is equivalent to compound **99** and when they are compared it is found the N_F phase is stabilised in compound **130**. However, when compound **131** is compared with compound **104**, instead the N_F phase is found to be destabilised slightly in compound **131**. Both compounds **130** and **131** are destabilised compared to RM734 due to the addition of the lateral methoxy and methyl groups, respectively, to the middle aromatic ring which decreases the shape anisotropy of the molecules. The addition of a second methyl group in the middle aromatic ring as seen for compound **132** sees the N_F phase completely lost much like was seen for compound **104** and presumably for a similar reason. Compounds **133**, **134** and **135** all have an increase in T_{NFI} compared to RM734 and the N_F phase was stabilised to a greater degree as more fluorines were substituted into the molecules. Interestingly, compounds **79.1** and **108** which are analogous to compounds **133** and **134**, respectively, have the conventional nematic phase preceding the N_F phase and this suggests that the additional lateral fluorines *ortho* to the terminal cyano group destabilise the N phase more than the N_F phase. Li *et al.*[19] also reported that for compound **136** replacing the methoxy group joined to the

middle aromatic ring with a fluorine sees the N_F stabilised presumably due to the combination of the more electron withdrawing nature of the fluorine allowing the molecules to pack together in a parallel orientation as well as the fluorine substituent being less sterically bulky than a methoxy group and so the shape anisotropy is increased. Furthermore, for compound **137** with a hydrogen as a terminal group, the stability of the N_F phase was increased even further with a transition almost 100 °C higher than that seen for RM734. The value of T_{NFI} for compound **137** is the same as that reported for compound **112**, highlighting that shortening the terminal chain and adding lateral fluorines to the molecular backbone is particularly favourable for the formation of the N_F phase when considering these molecular structures. Compounds **138**, **139** and **140** as a sequence show the effect of the fluorines *ortho* to the terminal cyano group on the stability of the N_F phase. Compound **138** is the equivalent of compound **58** but the transition temperature of the N_F phase is some 8 °C higher with the replacement of the terminal nitrophenyl by a difluorocyanophenyl. Both compounds do, however, show higher values for the N_F transition than RM734 due to the additional fluorine in the middle aromatic ring removing electron density from it. Removing one of the fluorines *ortho* to the terminal cyano group in compound **139** sees the conventional nematic phase emerge with the removal of some lateral bulk and, in addition, the N_F phase was destabilised by 8 °C compared to compound **138**. In compound **140** the *ortho* fluorines next to the terminal cyano group were replaced by methyl groups which dramatically lowered the value of T_{NFI} presumably due to the decrease in shape anisotropy associated with the larger size of the methyl group compared to a fluorine and because these groups donate electrons into the aromatic ring which would

ChemPlusChem

Review

doi.org/10.1002/cplu.202300726

Chemistry Europe
European Chemical
Societies Publishing

Table 15. The molecular structures, phase sequences and average dipole moments of compounds **116–128**.
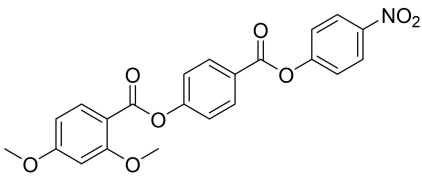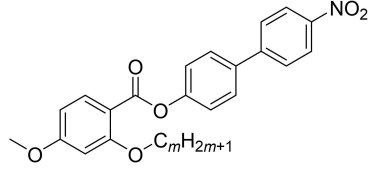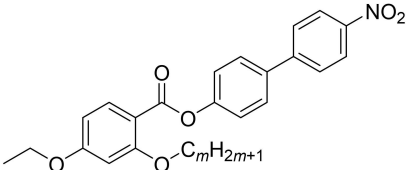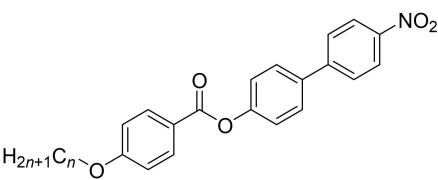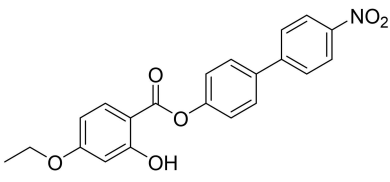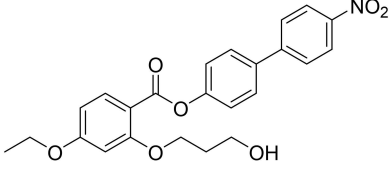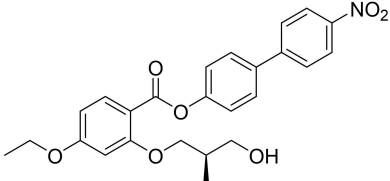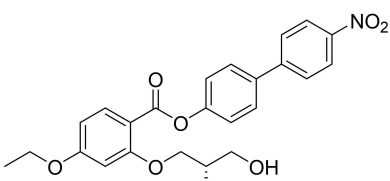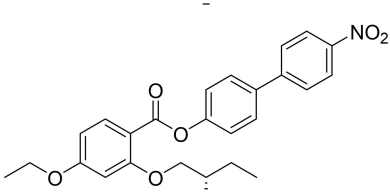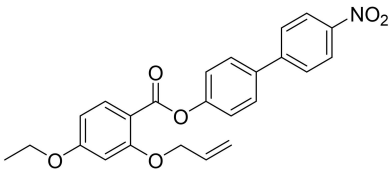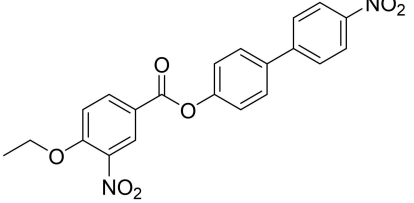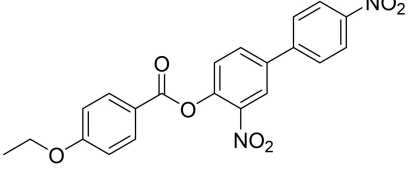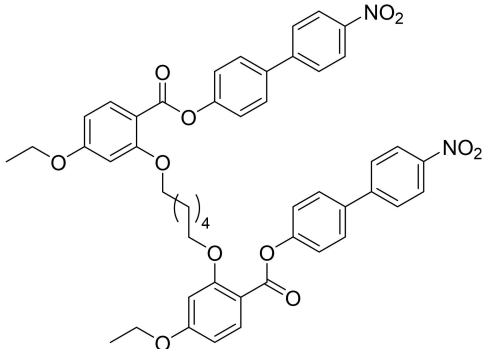
Compound		Structure	Melting Point/°C	Phase Sequence/°C	ΔT_{NF}/°C	μ/D	Ref.
52			140	I–188–N–133–N$_F$	–	11.4[a]	6,8
116	1		187	I–161–N	×	9.74[a]	42
	2		146	I–131–N	×	≈9.8[a]	42
117	1		152	I–166–N	×	10.0[a]	6,47
	2		151	I–109–N	×	≈10[a]	47
	3		138	I–79–N	×	≈10[a]	47
118	2		163	I–276–N	×	–	47
	3		144	I–218–N	×	–	47
119			175	I–215–N	×	–	47
120			158	I-96-N	×	–	47
121			163	I–94–N*	×	–	47
122			167	I–90–N*	×	–	47
123			97	I–42–N*	×	–	47

ChemPlusChem

Review
doi.org/10.1002/cplu.202300726

Chemistry Europe
European Chemical
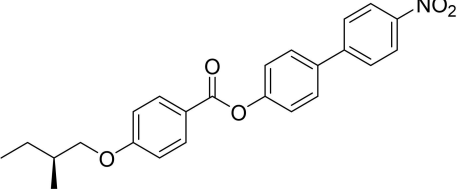Societies Publishing

Table 15. continued

Compound	Structure	Melting Point/°C	Phase Sequence/°C	ΔT_{NF}/°C	μ/D	Ref.
124		161	Cr–161–I	×	-	47
125		163	I–216–N*–197–SmA	×	–	47
126		187	Cr–187–I	×	–	47
127		161	I–146–N	×	–	47
128		207	Cr–207–I	×	–	47

[a] Calculated using B3LYP/6-31G (d).

increase the amplitude of the charge density wave at the end of the molecule which would be unfavourable for the N_F phase according to the modelling by Madhusudana.[52] Compound **141** replaces the lateral methoxy group in the terminal ring of compound **138** with the much bulkier CF_3 group and there is duly a decrease in the stability of the N_F phase. While the group can be accommodated laterally by the ferroelectric nematic molecules the bulk associated with it does appear to reduce the stability of the N_F phase compared to, for example, a lateral fluorine and this agrees with the observations made for the DIO–based compounds. Swapping the position of the CF_3 group to the middle ring as seen for compound **142**, sees the N_F phase destabilised by 10 °C compared to compound **141**,

suggesting that electronic factors are the driving force behind this destabilisation rather than shape effects. Series **143** and **144** also contain lateral CF_3 groups but in different positions along the molecule much like was described for compounds **141** and **142**. Much like was described earlier, as the terminal alkyloxy chain length was increased in both series the N_F phase was destabilised until in the case of **143.3** the phase was totally extinguished. Adding a second lateral CF_3 group to the molecular backbone in compound **145** sees a complete destabilisation of the N_F phase and it can be suggested that this is due to the bulk of these groups not being mitigated by the rest of the molecule. Li *et al*.[19] resolved the aforementioned issue in compound **146** by increasing the number of aromatic

ChemPlusChem

Review
doi.org/10.1002/cplu.202300726

Chemistry Europe
European Chemical
Societies Publishing

Table 16. The molecular structures, phase sequences and average dipole moments of compounds 129–151.
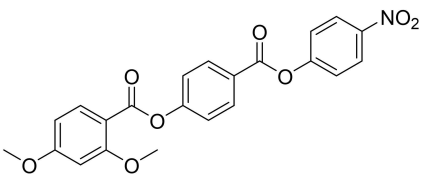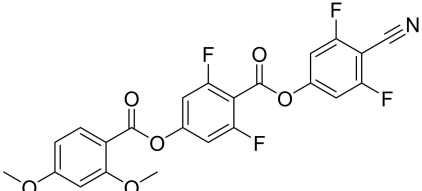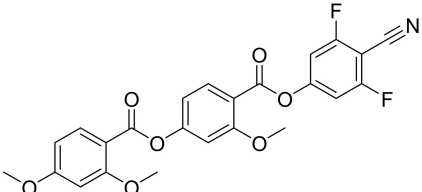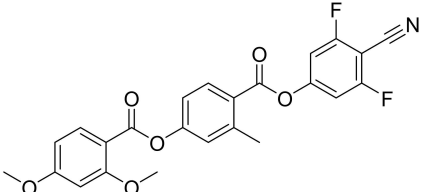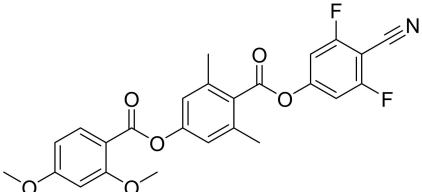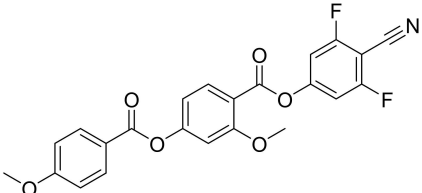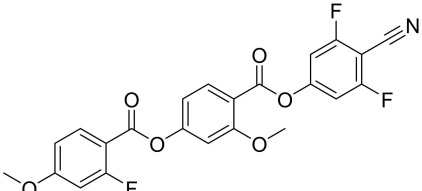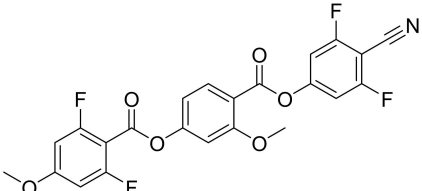
Compound	Structure	Melting Point/ °C	Phase Sequence/ °C	ΔT_{NF}/ °C	μ/D	Ref.
52		140	I–188–N–133–N$_F$	–	11.4[a]	6,8
129		–	I–162–N$_F$	+29	14.6[b]	19
130		–	I–107–N$_F$	−26	15.0[b]	19
131		–	I–107–N$_F$–82–Cr	−26	13.0[b]	19
132		–	I–84–Cr	×	12.4[b]	19
133		–	I–146–N$_F$–99–Cr	+13	13.8[b]	19
134		–	I–159–N$_F$–126–Cr	+26	14.4[b]	19
135		–	I–161–N$_F$–145–Cr	+28	14.5[b]	19

ChemPlusChem

Review
doi.org/10.1002/cplu.202300726

Chemistry
Europe
European Chemical
Societies Publishing
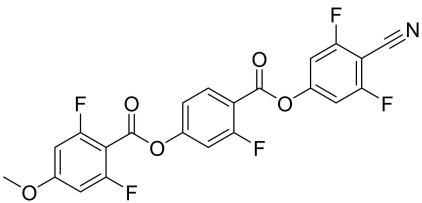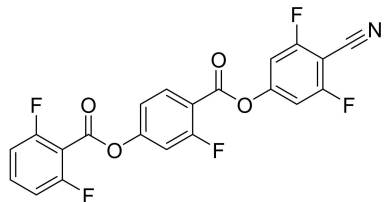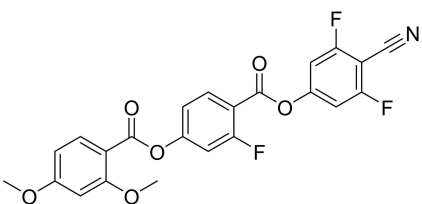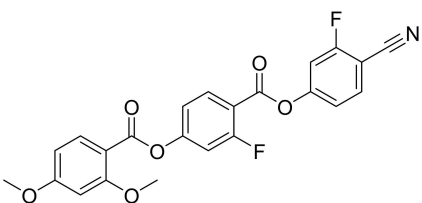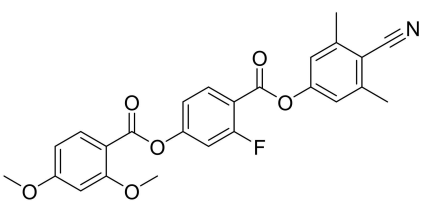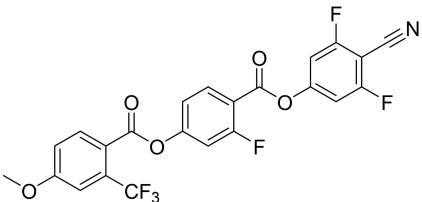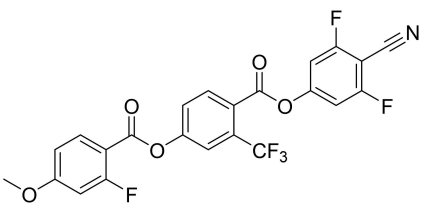
Compound	Structure	Melting Point/°C	Phase Sequence/°C	ΔT_{NF}/°C	μ/D	Ref.
136		–	I–200–N_F–153–Cr	+67	14.0[b]	19
137		–	I–229–N_F–145–Cr	+96	12.0[b]	19
138		–	I–151–N_F–131–Cr	+18	14.4[b]	19
139		–	I–166–N–143–N_F	+10	13.6[b]	19
140		–	I–76–N_F	−57	11.4[b]	19
141		–	I–111–N_F	−22	14.4[b]	19
142		–	I–101–N_F	−32	14.0[b]	19

Table 16. continued

ChemPlusChem

Review

doi.org/10.1002/cplu.202300726

Chemistry
Europe
European Chemical
Societies Publishing
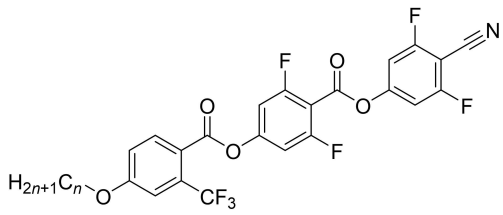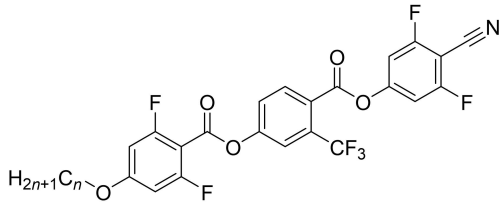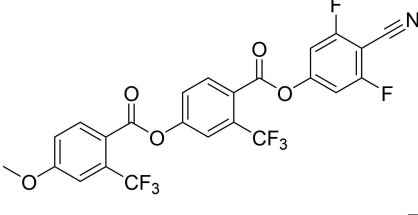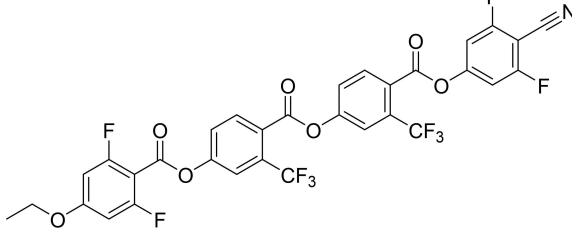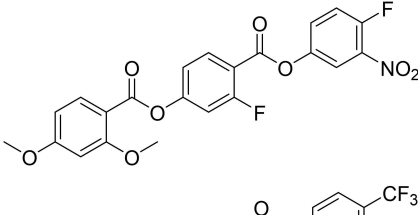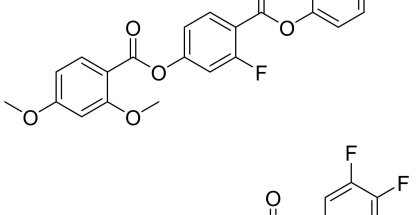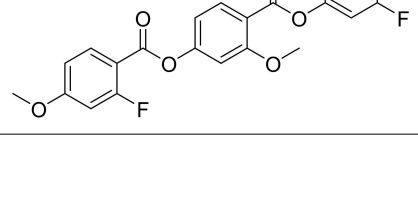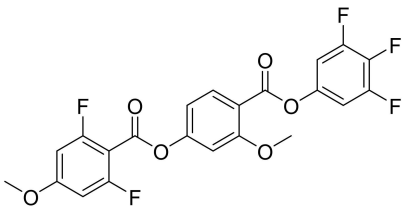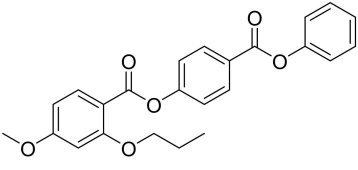
Table 16. continued

Compound		Structure	Melting Point/°C	Phase Sequence/°C	ΔT_{NF}/°C	μ/D	Ref.
143	1		–	I–106–N$_F$	−27	14.6[b]	19
	2		–	I–82–N–66–N$_F$	−67	15.1[b]	19
	3		–	I–57–N	×	15.3[b]	19
144	1		–	I–120–N$_F$	−13	14.0[b]	19
	2		–	I–84–N$_F$–51–Cr	−49	14.4[b]	19
145			–	I–105–Cr	×	13.7[b]	19
146			–	I–186–N–156–N$_F$	+23	17.1[b]	19
147			–	I–160–Cr	×	12.5[b]	19
148			–	I–91–Cr	×	10.4[b]	19
149			–	I–114–Cr	×	10.6[b]	19

Table 16. continued						
Compound	Structure	Melting Point/ °C	Phase Sequence/ °C	ΔT_{NF}/ °C	μ/D	Ref.
150		–	I–105–Cr	×	10.8[b]	19
151		–	I–61–Cr	×	6.0[b]	18
[a] Calculated using B3LYP/6-31G (d). [b] Calculated using B3LYP/6-311+G(d,p).						

rings to four while maintaining the two lateral CF_3 groups, and in this case the N_F phase was indeed observed despite the number of lateral substituents. This observation highlights that, the careful design of these ferroelectric nematogens can allow for their properties to be tailored depending on the different functionalities present.

Li *et al.*[19] also reported on other terminal functionality than just the difluorocyanophenyl moiety including the transitional behaviour of compound **147**. In this case the terminal functionality of compound **59** was swapped so that the nitro group was now *meta* to the ester in the terminal ring and the fluorine was *para* to the ester. These modifications, while keeping a larger longitudinal dipole moment of 12.5 D, did see the N_F phase extinguished unlike compound **59** presumably due to the enhanced lateral bulk with the *meta* position of the nitro group. They also described compounds **148**, **149** and **150** in which the terminal group was replaced and in all three of these materials the N_F phase was not observed, in fact they were completely non–mesogenic. Li *et al.*[18] had also previously shown that removing the polar terminal group from compound **61.3**, as seen with compound **151**, saw a large decrease in the molecular dipole and unsurprisingly the N_F phase was not observed.
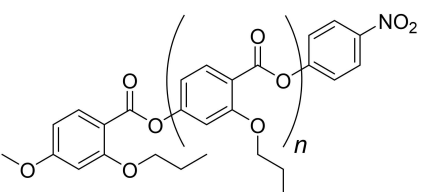
Summarising what effect different modifications have on the stability of the N_F phase for the materials based on RM734 a number of observations can be made. Increasing the chain length of both lateral and terminal chains causes the N_F phase to be destabilised, however, this is to a greater extent for the terminal chain and this can be rationalised using the model proposed for the N_F phase by Madhusudana.[52] Critically having no terminal chain or functionality saw the N_F phase maintained whereas when the lateral groups were removed or replaced by OH groups, for example, the N_F phase was extinguished. Adding a chiral group laterally in the RM734 template gave rise to the chiral N_F phase. But adding additional lateral groups such as seen with compounds **99** and **104** saw the conventional nematic phase destabilised such that direct N_F–I transitions

were seen, although further additions also saw the N_F phase completely destabilised as well. Indeed, while bulky lateral functionality such as CF_3 groups could be added to the molecule and the N_F phase maintained, these additions saw the N_F phase destabilised because of the decrease in shape anisotropy. Opposingly, replacing the terminal nitrophenyl moiety with a nitrobiphenyl moiety saw the N_F and N phases both stabilised presumably due to the increase in shape anisotropy and enhanced interactions between the molecules. Madhusudana's model can also be used to justify the stabilisation of the N_F phase with the addition of fluorine atoms *ortho* to the terminal nitro group or laterally along the backbone of the molecule. When the backbone of the molecule was heavily fluorinated and the terminal nitrophenyl moiety was replaced by a difluorocyanophenyl moiety the N_F phase was found to be particularly stabilised reaching transition temperatures of over 200 °C. However, replacing the terminal aromatic functionality with any groups other than a nitro or cyano proved to extinguish the N_F phase and this was similarly seen if one of the ester groups of a material in the RM734 family was removed, regardless of the rest of the functionality present within the molecule.

5. Other Potential N_F Compounds

In Table 17, higher oligomers are reported which have structures similar to that found in the RM734 family, and these were investigated in order to determine if the N_F phase was exclusive to low molar mass materials. Mandle *et al.*[47] reported the tetramer which is shown by compound **152** but this was completely non–mesogenic. Li *et al.*[25] described two series of polymers in which the number of middle aromatic rings were increased with series **153** being terminated by a benzyl moity and series **154** by a nitrophenyl moiety. These series appear to be more conducive for maintaining the large longitudinal dipole moment seen for other ferroelectric nematogens than

ChemPlusChem

Review

doi.org/10.1002/cplu.202300726

Chemistry
Europe
European Chemical
Societies Publishing

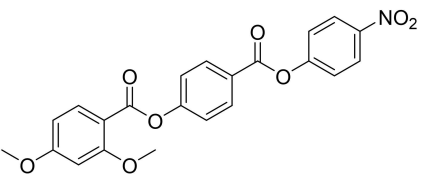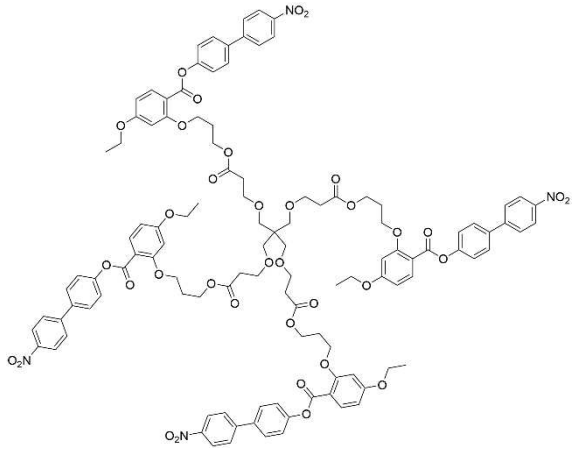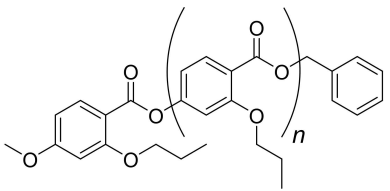**Table 17.** The molecular structures, phase sequences and average dipole moments of compounds **152–154**.

Compound	Structure	Melting Point/ °C	Phase Sequence/ °C	ΔT_{NF}/ °C	μ/D	Ref.
52		140	I–188–N–133–N$_F$	–	11.4[a]	6,8
152		56	Cr–56–I	×	–	47
153 2		–	Cr–110–I	×	8.9[a]	25
3		–	Cr–138–I	×	11.0[a]	25
4		–	I–60–Cr	×	15.7[a]	25
6		–	I–184–N$_F$–135–Cr	+51	21.5[a]	25
8		–	I–230–N$_F$–167–Cr	+97	–	25
10		–	I–264–N$_F$–192–Cr	+131	–	25
12		–	I–294–N$_F$–210–Cr	+161	–	25
154 1		–	I–41–N$_F$	–92	12.4[a]	25
2		–	I–116–N$_F$	–17	15.8[a]	25
3		–	I–165–N$_F$–35–G	+22	18.9[a]	25
4		–	I–207–N$_F$–40–G	+74	21.4[a]	25
6		–	I–265–N$_F$–137–Cr	+132	27.2[a]	25
8		–	I–284–N$_F$–171–Cr	+151	33.5[a]	25
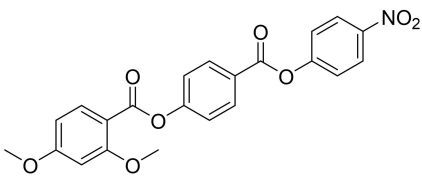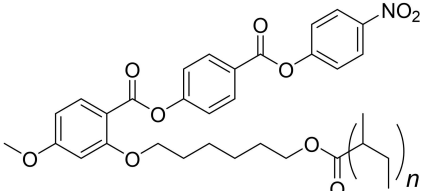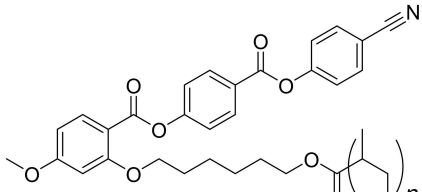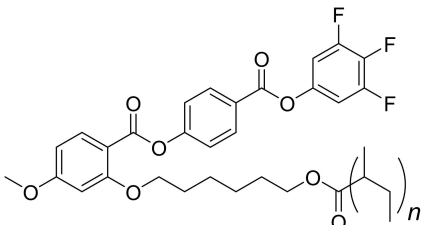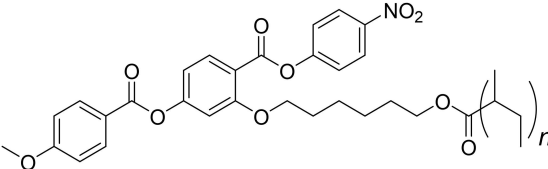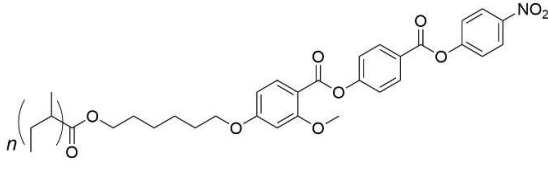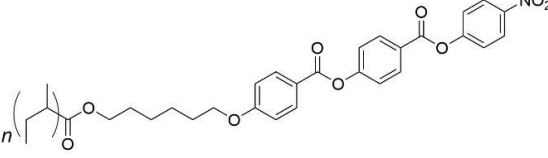
[a] Calculated using B3LYP/6-31G (d).

for example compound **152**. When the number of monomeric units in series **153** are low, the N$_F$ phase is not observed, however, when $n \geq 6$ the phase emerges. While both series have somewhat extensive lateral bulk, with propoxy chains connected to both the middle aromatic rings and to the terminal ring which contains the methoxy group, the addition of extra aromatic rings when n increased is presumably a stronger driving force for the transition temperatures. All four members of series **153** which exhibit the N$_F$ phase, had their phase transitions at higher temperatures than RM734. As the number of monomeric units within the molecular structure increased, so did both the average molecular dipole moment and the reported values of T$_{NFI}$. T$_{NFI}$ for compound **153.12** was stabilised by some 161 °C compared to RM734 and this is the highest transition temperature for the N$_F$ phase reported to

date. Series **154** exhibited similar behaviour to series **153** with the dipole moments of the constituent members and their transition temperatures increasing as the value of n likewise increased. Unlike series **153**, all members of series **154** exhibited the N$_F$ phase, although for compound **154.1** the N$_F$ phase was destabilised compared to RM734 by 92 °C presumably because of the lateral propoxy groups lowering the shape anisotropy and this not being mitigated fully by the enhanced number of aromatic rings as seen for the higher values of n. Series **154** shows higher values of T$_{NFI}$ than series **153** when the homologues with the same values of n are compared presumably due to the enhanced polarizability endowed by the terminal nitrophenyl moiety.

In Table 18, side–chain polymers which are based on RM734 are reported, with Dai *et al.*[44] describing a number of these

ChemPlusChem

Review
doi.org/10.1002/cplu.202300726

Chemistry Europe
European Chemical
Societies Publishing

Table 18. The molecular structures, phase sequences and average dipole moments of compounds **155–160**.

Compound	Structure	Melting Point/ °C	Phase Sequence/°C	ΔT_{NF}/ °C	μ/D	Ref.
52		140	I–188–N–133–N_F	–	11.4[a]	6,8
155		–	I–122–N–80–N_F–44–G	−53	11.8[a]	44
156		–	I–92–N–43–G	×	11.6[a]	44
157		–	I–52–G	×	9.0[a]	44
158		–	I–39–G	×	–	44
159		–	N–212–SmA–44–G	×	–	44
160		–	I/N–250–SmA–37–G	×	–	44

[a] Calculated using B3LYP/6-31G (d).

materials with large dipole moments as shown by compounds **155** to **160**. Compounds **156**, **157** and **158** had the polymer backbone connected to the highly polar moiety in a lateral position. Compound **156** was terminated by a nitrophenyl moiety and exhibited the N_F phase highlighting the

ability of these material to withstand large lateral substituents in this position. The value of T_{NFN} was 53 °C lower than that observed for RM734, critically however, this showed that a side–chain polymer exhibited the N_F phase and was another example of a material which in this class which could not be described

as a standard low molar mass mesogen. Compounds **156** and **157** had the terminal nitrophenyl moiety replaced by cyanophenyl and trifluorophenyl moieties, respectively, and in both cases the N_F phase was extinguished. This was similarly seen for compounds **66.1** and **67.1** which had the same changes in the terminal functionality when they were compared to RM734. Compound **158** saw the ether link to the polymer moved to the middle aromatic ring and the N_F phase was completely destabilised. Somewhat surprisingly considering the observation of the N_F phase for all the members of series **79**, Dai et al.[44] suggested that the N_F phase was not observed because of the packing of the polar moieties within the polymer side chains which favoured anti–parallel contacts which destabilise the N_F phase. The molecular packing of compounds **159** and **160** can also explain the phase behaviour of those polymers, with both materials exhibiting the conventional smectic A phase rather than the N_F phase. With the promotion of head–to–head anti–parallel packing in both compounds promoting a layered structure which gave no overall polarity.

Table 19 contains a range of compounds exhibiting the N_F phase but do not truly fit into any of the archetypal families of compounds listed in the introduction. They are, however, still low molar mass materials with large longitudinal dipole moments and some degree of lateral bulk. They possess some features in terms of their molecular structures which can be related to the other compounds which have been reported previously but with key differences. Compound **161** had a highly rigid construction which is terminated with a dioxane ring like DIO but instead of an ester had an alkynyl bond. The other terminus of the compound has a highly fluorinated biphenyl capped by a cyano group to give it the aforementioned large molecular dipole moment of 14 D. Song et al.[31] reported that compound **161** exhibited both the N_F and the SmA_F phases much like compound **25.3** which had similar structural features. Li et al.[19] described compound **162** in which the dioxane ring was replaced by a terminal butyl chain akin to that seen for UUQU-4 N but in this case the N_F phase was totally destabilised. This suggests that the dioxane ring has a key role in stabilising the N_F phase when there is terminal bulk being added to these materials. Song et al.[41] had previously reported on another set of highly fluorinated rigid compounds with large longitudinal dipole moments namely compounds **163** and **164**. Compound **163** has a similar molecular structure to compound **161** but with the triple bond linking group removed, however, this material does still exhibit the N_F phase. The value of T_{NFNX} in compound **163** is 2°C higher than that of compound **161** which suggests that the alkynyl bond has a limited effect on the stability of the N_F phase overall. Increasing the length of the terminal chain, as seen for compound **164**, has the same effect as has been described earlier in this review, with the N_F phase being completely destabilised. Nishikawa et al.[51] reported that replacing the terminal dioxane ring in compound **161** with a bicyclo–orthoester to give series **165**, sees the N_F phase stabilised by over 100°C to give values of T_{NFI} of nearly 300°C which are some of the highest values seen for these transitions which are enantiotropic in nature. This increase in stability is presumably due to the enhanced rigidity

of the molecule endowed by the tolane linking group and the terminal bicyclo–orthoester. Despite having a different molecular structure to the other archetypal families of ferroelectric nematogens, the fact that these compounds show similar trend in transition temperatures with regards to these terminal chain length means that again this can be attributed to the modelling described by Madhususdana.[52] These materials show that even if the materials deviate a little more from the archetypal templates they still can exhibit the N_F phase.
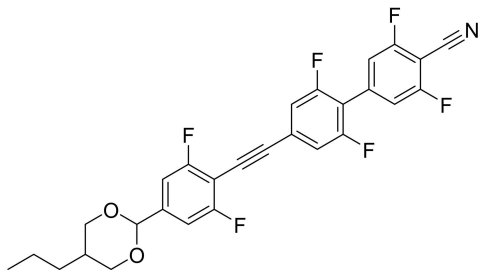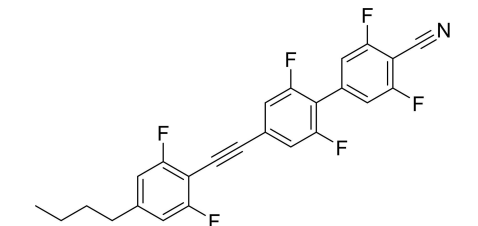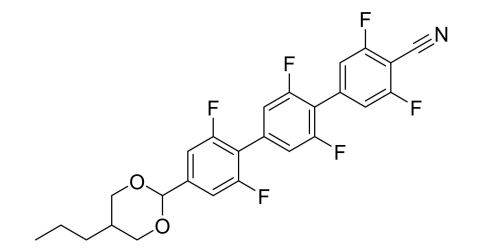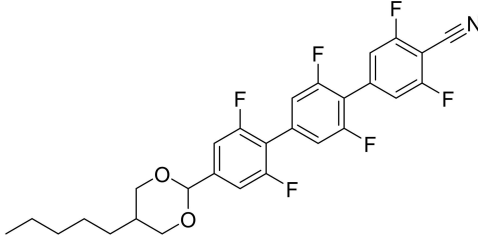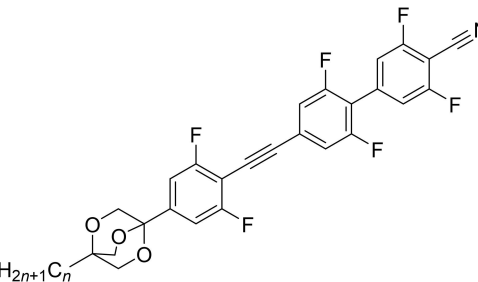
Adding additional middle aromatic rings as shown by series **153** and **154** to form polymers saw the N_F phase stabilised as the number of monomeric units within the molecule increased presumably due to the increase in lateral interactions between the dipoles promoting parallel correlations. The RM734 template also can be used for making side–chain polymers but in that case the N_F phase was only seen when the chain was connected to the terminal ring with the methoxy group in a lateral position. One area that was critical to seeing the conventional nematic phase having a wider appeal was that the archetypal room temperature nematogens, the nCB series,[1] could be mixed to tune the properties of the mixtures to better suit electrooptic applications. The N_F phase could in the future see a similar tuning by using those materials in mixtures. There have been examples of N_F mixtures in literature,[29,36,37,41,42,49,53,60,62–66] but it must be highlighted that the N_F phase has shown that it can withstand non–mesogenic dopants to enhance particular properties such as the nonlinear optical susceptibility.[12,67]

6. Conclusions

The ferroelectric nematic phase, as was alluded to in the introduction of this review, has proven itself to be one of the most exciting topics of research in the field of liquid crystals. The structure space that these materials exist in has been relatively small to date, but the utilisation of neural networks as outlined by Mandle[55] has provided a method which could process vast libraries of prospective compounds while reducing human bias. However, using such a technique does not reduce the time required for the synthesis of the compounds or their characterisation and so that remains the major time impediment.

Considering the N_F materials which have been studied in literature there are a number of observations that can be made around their molecular structures as well as what effect structural modifications have on the stability of the phase. In DIO one of the key structural features is the terminal dioxane ring, with the replacement of this by a butoxy chain leading to the N_F phase being extinguished. The group has a significant effect on the overall molecular dipole while also endowing enhanced steric bulk to the terminal of the molecule, which presumably helps to inhibit the molecules from packing in an anti–parallel manner because it fills void space less efficiently. Increasing the length of this terminal chain starts to then disrupt the packing of the mesogenic units and changes the electronic profile of that terminal region. Therefore, the length

Table 19. The molecular structures, phase sequences and average dipole moments of compounds **161–165**.

Compound		Structure	Melting Point/°C	Phase Sequence/°C	μ/D	Ref.
161			140	N–202–N_X–185–N_F–120–SmA_{F-}	14.0[a]	31
162			–	I–143–N–104–Cr	11.8[b]	19
163			184	I–220–N–196–N_X–187–N_F–158–Cr	13.6[b]	41
164			162	I–208–N–151–N_X–137–Cr	13.7[b]	41
165	**1**		219	I–291–N_F	15.0[b]	51
	2		197	I–289–N_F	15.2[b]	51

[a] Calculated using B3LYP/6-31G (d). bCalculated using B3LYP/6-311+G(d,p).

of the alkyl chain, which is bonded to this dioxane ring, or in the case of RM734-type materials to the terminal position of the aromatic ring system, is a strong driver of the stability of the N_F phase. This observation can be rationalised using the model proposed by Madhusudana[52] due to the influence changing the alkyl chain length has on the electron density of the terminal aromatic ring as well as dilution effects.

In general, the materials which exhibit the N_F phase see the phase destabilised when the size of the lateral groups increases

either through using lateral alkyloxy chains or other functionalities. With this observation presumably being shape driven since the decrease in the shape anisotropy of the molecules is less favourable for the interactions between the mesogenic units. There is an exception to this in that adding fluorines laterally along the molecular backbone seems to be favourable for the exhibition of the N_F phase. Presumably this is because the shape and electronic effects of adding these fluorines is dominated by the electronic effects which sees an

ChemPlusChem

Review

doi.org/10.1002/cplu.202300726

Chemistry
Europe
European Chemical
Societies Publishing

enhancement in the overall dipole moment as well as in the electron density within each of the aromatic rings such that the molecules pack preferentially into the N$_F$ phase considering Madhusudana's model.[52] One method which can be used in particular to stabilise the N$_F$ phase is to have a polar group in the terminal position of the aromatic ring system with fluorines *ortho* to it. The polar group is able to generate the large overall dipole which is often seen for this type of materials and the fluorines spread the negative charge at the terminal of the molecule which removes electron density from the nitro group helping to stabilise the ferroelectric nematic phase.

Although in UUQU-4N style materials the linking group is that of a difluoromethyl moiety and these materials can exhibit the N$_F$ phase, overall, the replacement of the ester linking group by this moiety is unfavourable for the stability of the N$_F$ phase. Presumably this is because the distribution of the electron density within the molecule is less favourable than when it is divided by an ester group which means that the parallel alignment of the calamitic molecules is less favourable and then the N$_F$ phase is destabilised. Indeed, most modifications made to the archetypal N$_F$ materials sees the phase destabilised and in many cases the N$_F$ is completely extinguished. This is presumably because the stability of the N$_F$ phase is related to both shape effects and electronic effects, and this means that many modifications will see a promotion in the unfavourable anti–parallel correlations or will have lateral bulk such that the interactions between the mesogenic units are diluted.

It must be noted, however, that the N$_F$ phase is able to withstand the introduction of key functionalities to, for example, the RM734 template, even if it is destabilised, such as lateral chiral groups including the chiral 2-methylbutoxy moiety to give the helielectric nematic phase/chiral ferroelectric nematic phase. Similarly, this can be taken advantage of to add a lateral acrylate moiety which allows a polymeric compound to show the N$_F$ phase whereas this introduction of this moiety in other positions on the molecular backbone merely yields conventional nematic and smectic phases and not the ferro-electric nematic phase. One area that appears to be of great promise in terms of polymeric N$_F$ materials are the compounds in which the number of aromatic rings in the middle of the molecule along the long axis of the molecule is increased, which increases the stability of the N$_F$ phase, and this allows for the possibility of including different more exotic lateral groups while still maintaining the desired N$_F$ phase. This general principle can also be applied to low molar mass materials, where again increasing the number of aromatic rings within the molecule sees the N$_F$ phase be stabilised.

This field is an area of constant advancement which is what makes it so exciting to study as a chemist and to try to design new materials which harness such a fascinating phase. During the writing of this review, this was highlighted by the reporting of another example of a enantiotropic ferroelectric nematogen by Karcz *et al.*[68] in a material somewhat similar to compound **29**. Stepanafas *et al.* reported on the effect of replacing the terminal methoxy group with a terminal methylthio group with respect to the N$_F$ phase while also sequentially changing the degree of fluorination incorporated into the molecular

backbone.[69] Gibb *et al.* reported a series of ferroelectric nematogens which were synthesised without using a protecting intermediate, and of particular note is the observation of the N$_F$ phase in a material where the terminal methoxy group was replaced by an iodine.[70] Cruickshank *et al.* also reported a range of RM734-type compounds with multiple lateral groups which exhibited direct N$_F$–I transitions.[71] As these recent additions to the literature show, the ferroelectric nematic phase remains the hottest topic in the field of liquid crystals, and new molecules continue to be synthesised which exhibit the phase. Furthermore, as the theoretical understanding of this phase improves, this exciting polar continues to have a very golden future.

Conflict of Interests

There are no conflicts to declare.

[1] G. W. Gray, K. J. Harrison, J. A. Nash, *Electron. Lett.* **1973**, *9*, 130–131.
[2] M. Born, *Sitzungsber. Preuss. Akad Wiss.* **1916**, *30*, 614–650.
[3] N. Scaramuzza, G. Strangi, C. Versace, *Liq. Cryst.* **2001**, *28*, 307–312.
[4] T. J. Sluckin, D. A. Dunmur, H. Stegemeyer, *Crystals That Flow: Classic Papers From the History of Liquid Crystals.* **2004**, pp. 512 CRC Press, Boca Raton.
[5] R. J. Mandle, S. J. Cowling, J. W. Goodby, *Phys. Chem. Chem. Phys.* **2017**, *19*, 11429–11435.
[6] R. J. Mandle, S. J. Cowling, J. W. Goodby, *Chem. A Eur. J.* **2017**, *23*, 14554–14562.
[7] H. Nishikawa, K. Shiroshita, H. Higuchi, Y. Okumura, Y. Haseba, S. I. Yamamoto, K. Sago, H. A. Kikuchi, *Adv. Mater.* **2017**, *29*, 1702354.
[8] X. Chen, E. Korblova, D. Dong, X. Wei, R. Shao, L. Radzihovsky, M. A. Glaser, J. E. Maclennan, D. Bedrov, D. M. Walba, N. A. Clark, *Proc. Nat. Acad. Sci.* **2020**, *117*, 14021–14031.
[9] F. Caimi, G. Nava, R. Barboza, N. A. Clark, E. Korblova, D. M. Walba, T. Bellini, L. Lucchetti, *Soft Matter.* **2021**, *17*, 8130–8139.
[10] P. Rudquist, *Sci. Rep.* **2021**, *11*, 24411.
[11] N. Sebastián, L. Cmok, R. J. Mandle, M. R. De La Fuente, I. Drevenšek O-lenik, M. Čopič, A. Mertelj, *Phys. Rev. Lett.* **2020**, *124*, 037801.
[12] C. L. Folcia, J. Ortega, R. Vidal, T. Sierra, J. Etxebarria *Liq. Cryst.* **2022**, *49*, 899–906.
[13] J. Ortega, C. L. Folcia, J. Etxebarria, T. Sierra, *Liq. Cryst.* **2022**, *49*, 2128–2136.
[14] D. Pociecha, R. Walker, E. Cruickshank, J. Szydlowska, P. Rybak, A. Makal, J. Matraszek, J. M. Wolska, J. M. D. Storey, C. T. Imrie, E. Gorecka, *J. Mol. Liq.* **2021**, *361*, 119532.
[15] E. Zavvou, M. Klasen-Memmer, A. Manabe, M. Bremer, A. Eremin, *Soft Matter.* **2022**, *18*, 8804–8812.
[16] H. Nishikawa, K. Sano, S. Kurihara, G. Watanabe, A. Nihonyanagi, B. Dhara, F. Araoka, *Commun. Mater.* **2022**, *3*, 89.
[17] X. Chen, E. Korblova, M. A. Glaser, J. E. MacLennan, D. M. Walba, N. A. Clark, *Proc. Natl. Acad. Sci. USA* **2021**, *118*, e2104092118.
[18] J. Li, H. Nishikawa, J. Kougo, J. Zhou, S. Dai, W. Tang, X. Zhao, Y. Hisai, M. Huang, S. Aya, *Sci. Adv.* **2021**, *7*, eabf5047.

ChemPlusChem

Review

doi.org/10.1002/cplu.202300726

Chemistry
Europe

European Chemical
Societies Publishing

[19] J. Li, Z. Wang, M. Deng, Y. Zhu, X. Zhang, R. Xia, Y. Song, Y. Hisai, S. Aya, M. Huang, *Giant.* **2022**, *11*, 100109.

[20] R. Saha, P. Nepal, C. Feng, M. S. Hossain, M. Fukuto, R. Li, J. T. Gleeson, S. Sprunt, R. J. Twieg, A. Jákli, *Liq. Cryst.* **2022**, *49*, 1784–1796.

[21] S. Brown, E. Cruickshank, J. M. D. Storey, C. T. Imrie, D. Pociecha, M. Majewska, A. Makal, E. Gorecka, *ChemPhysChem.* **2021**, *22*, 2506–2510.

[22] H. Nishikawa, K. Sano, F. Araoka, *Nat. Commun.* **2022**, *13*, 1142.

[23] R. J. Mandle, N. Sebastián, J. Martinez-Perdiguero, A. Mertelj, *Nat. Commun.* **2021**, *12*, 4962.

[24] A. Manabe, M. Bremer, M. Kraska, *Liq. Cryst.* **2021**, *48*, 1079–1086.

[25] J. Li, R. Xia, H. Xu, J. Yang, X. Zhang, J. Kougo, H. Lei, S. Dai, H. Huang, G. Zhang, F. Cen, Y. Jiang, S. Aya, M. Huang, *J. Am. Chem. Soc.* **2021**, *143*, 46.

[26] N. Vaupotič, D. Pociecha, P. Rybak, J. Matraszek, M. Čepič, J. Wolska, E. Gorecka, *Liq. Cryst.* **2023**, *50*, 584–595.

[27] A. Erkoreka, J. Martinez-Perdiguero, R. J. Mandle, A. Mertelj, N. Sebastián, *J. Mol. Liq.* **2023**, *387*, 122566.

[28] H. Nishikawa, F. A. Araoka, *Adv. Mater.* **2021**, *33*, 2101305.

[29] X. Chen, Z. Zhu, M. J. Magrini, E. Korblova, C. S. Park, M. A. Glaser, J. E. Maclennan, D. M. Walba, N. A. Clark, *Liq. Cryst.* **2022**, *49*, 1531–1544.

[30] N. Sebastián, R. J. Mandle, A. Petelin, A. Eremin, A. Mertelj, *Liq. Cryst.* **2021**, *48*, 2055–2071.

[31] Y. Song, M. Deng, Z. Wang, J. Li, H. Lei, Z. Wan, R. Xia, S. Aya, M. Huang, *J. Phys. Chem. Lett.* **2022**, *13*, 9983–9990.

[32] C. Feng, R. Saha, E. Korblova, D. Walba, S. N. Sprunt, A. Jákli, C. Feng, S. N. Sprunt, A. Jákli, R. Saha, E. Korblova, D. Walba, *Adv. Opt. Mater.* **2021**, *9*, 2101230.

[33] N. Tufaha, E. Cruickshank, D. Pociecha, E. Gorecka, J. M. D. Storey, C. T. Imrie, *Chem. A Eur. J.* **2023**, *29*, e202300073.

[34] R. Berardi, M. Ricci, C. Zannoni, *Ferroelectrics* **2004**, *309*, 3–13.

[35] R. Berardi, M. Ricci, C. Zannoni, *ChemPhysChem.* **2001**, *2*, 443–447.

[36] J. Zhou, R. Xia, M. Huang, S. Aya, *J. Mater. Chem. C* **2022**, *10*, 8762–8766.

[37] E. Cruickshank, R. Walker, J. M. D. Storey, C. T. Imrie, *RSC Adv.* **2022**, *12*, 29482–29490.

[38] H. Kikuchi, H. Matsukizono, K. Iwamatsu, S. Endo, S. Anan, Y. Okumura, *Adv. Sci.* **2022**, *9*, 2202048.

[39] R. J. Mandle, *Soft Matter.* **2022**, *18*, 5014–5020.

[40] N. Sebastián, M. Čopič, A. Mertelj, *Phys. Rev. E.* **2022**, *106*, 021001.

[41] Y. Song, J. Li, R. Xia, H. Xu, X. Zhang, H. Lei, W. Peng, S. Dai, S. Aya, M. Huang, *Phys. Chem. Chem. Phys.* **2022**, *24*, 11536–11543.

[42] E. Cruickshank, A. Pearson, S. Brown, J. M. D. Storey, C. T. Imrie, R. Walker, *Liq. Cryst.* **2023**, *50*, 1960–1967.

[43] R. J. Mandle, *Liq. Cryst.* **2022**, *49*, 2019–2026.

[44] S. Dai, J. Li, J. Kougo, H. Lei, S. Aya, M. Huang, *Macromolecules* **2021**, *54*, 6045–6051.

[45] H. Matsukizono, K. Iwamatsu, S. Endo, Y. Okumura, S. Anan, H. Kikuchi, *J. Mater. Chem. C* **2023**, *11*, 6183–6190.

[46] A. Mertelj, L. Cmok, N. Sebastián, R. J. Mandle, R. R. Parker, A. C. Whitwood, J. W. Goodby, M. Čopič, *Phys. Rev. X* **2018**, *8*, 041025.

[47] R. J. Mandle, S. J. Cowling, J. W. Goodby, *Liq. Cryst.* **2021**, *48*, 1780–1790.

[48] S. Nishimura, S. Masuyama, G. Shimizu, C.-Y. Chen, T. Ichibayashi, J. Watanabe, *Adv. Phys. Res.* **2022**, *1*, 2200017.

[49] X. Chen, V. Martinez, E. Korblova, G. Freychet, M. Zhernenkov, M. A. Glaser, C. Wang, C. Zhu, L. Radzihovsky, J. E. Maclennan, D. M. Walba, N. A. Clark, *Proc. Nat. Acad. Sci.* **2022**, *120*, e2217150120.

[50] E. Cruickshank, P. Rybak, M. M. Majewska, S. Ramsay, C. Wang, C. Zhu, R. Walker, J. M. D. Storey, C. T. Imrie, E. Gorecka, D. Pociecha, *ACS Omega* **2023**, *8*, 36562–36568.

[51] H. Nishikawa, F. Araoka, D. Stéfani Teodoro Martinez, R. Furlan de Oliveira, H. Nishikawa, M. Kuwayama, A. Nihonyanagi, B. Dhara, *J. Mater. Chem. C* **2023**, *11*, 12525–12542.

[52] N. V. Madhusudana, *Phys. Rev. E.* **2021**, *104*, 014704.

[53] X. Chen, V. Martinez, P. Nacke, E. Korblova, A. Manabe, M. Klasen-Memmer, G. Freychet, M. Zhernenkov, M. A. Glaser, L. Radzihovsky, J. E. Maclennan, D. M. Walba, M. Bremer, F. Giesselmann, N. A. Clark, N. Abbott, P. Palffy-Muhoray, *Proc. Nat. Acad. Sci.* **2022**, *119*, e2210062119.

[54] P. Kirsch, W. Binder, J. Hahn, K. Jährling, M. Lenges, L. Lietzau, D. Maillard, V. Meyer, E. Poetsch, A. Ruhl, G. Unger, R. Fröhlich, *Eur. J. Org. Chem.* **2008**, *2008*, 3479–3487.

[55] R. J. Mandle, *Liq. Cryst.* **2023**, *50*, 534–542.

[56] W. Weissflog, D. Demus, *Cryst. Res. Technol.* **1983**, *18*, K21–K24.

[57] W. Weissflog, D. Demus, *Cryst. Res. Technol.* **1984**, *19*, 55–64.

[58] M. Cigl, N. Podoliak, T. Landovský, D. Repček, P. Kužel, V. Novotná, *J. Mol. Liq.* **2023**, *385*, 122360.

[59] J. Szydlowska, P. Majewski, M. Čepič, N. Vaupotič, P. Rybak, C. T. Imrie, R. Walker, E. Cruickshank, J. M. D. Storey, P. Damian, E. Gorecka, *Phys. Rev. Lett.* **2023**, *130*, 216802.

[60] X. Zhao, J. Zhou, J. Li, J. Kougo, Z. Wan, M. Huang, S. Aya, *Proc. Natl. Acad. Sci. USA* **2021**, *118*, e2111101118.

[61] G. J. Strachan, W. T. A. Harrison, J. M. D. Storey, C. T. Imrie, *Phys. Chem. Chem. Phys.* **2021**, *23*, 12600–12611.

[62] H. Long, J. Li, M. Huang, S. Aya, *Liq. Cryst.* **2022**, *49*, 2121–2127.

[63] X. Zhao, H. Long, H. Xu, J. Kougo, R. Xia, J. Li, M. Huang, S. Aya, *Proc. Natl. Acad. Sci. USA* **2022**, *119*, e2205636119.

[64] H. Kamifuji, K. Nakajima, Y. Tsukamoto, M. Ozaki, H. Kikuchi, *Appl. Phys. Express* **2023**, *16*, 071003.

[65] J. Zhou, Y. Zou, J. Li, M. Huang, S. Aya, *PNAS Nexus* **2023**, *2*, 265.

[66] X. Zhao, J. Li, M. Huang, S. Aya, *J. Mater. Chem. C* **2023**, *11*, 8547–8552.

[67] R. Xia, X. Zhao, J. Li, H. Lei, Y. Song, W. Peng, X. Zhang, S. Aya, M. Huang, *J. Mater. Chem. C* **2023**, *11*, 10905–10910.

[68] J. Karcz, N. Rychłowicz, M. Czarnecka, A. Kocot, J. Herman, P. Kula, *Chem. Commun.* **2023**, *59*, 14807–14810.

[69] G. Stepanafas, E. Cruickshank, S. Brown, M. M. Majewska, D. Pociecha, E. Gorecka, J. M. D. Storey, C. T. Imrie, *Mater Adv* **2023**, *5*, 525–538.

[70] C. J. Gibb, R. J. Mandle, *J. Mater. Chem. C* **2023**, *11*, 16982–16991.

[71] E. Cruickshank, N. Tufaha, R. Walker, S. Brown, E. Gorecka, D. Pociecha, J. M. D. Storey, C. T. Imrie, *Liq. Cryst.* **2024**, DOI: 10.1080/02678292.2024.2304598.